Chapter 4
Fracture of Materials Loaded Along Cracks: Approach and Results

Viacheslav Bogdanov, Aleksander Guz, and Vladimir Nazarenko

4.1 Introduction

Technological processes of manufacturing structural materials and assembling structure elements made of them often generate fields of initial (residual) stresses and strains in such materials. Those initial stresses must be taken into account in the calculations of product strength and durability, especially if crack-like defects emerge in such products in the processes of their manufacturing and operation. In the situation when initial stresses act along crack surfaces (and this situation is typical, e.g., in laminar or unidirectional fibrous composites (Dvorak 2000; Malmeister et al. 1980; Shul'ga and Tomashevskii 1997), materials with thermal insulation or anticorrosion coatings) (Ainsworth et al. 2000), the approaches of classical fracture mechanics (Cherepanov 1979; Kassir and Sih 1975) prove to be inapplicable. This results from the fact that such initial stresses are not involved in the expressions for stress intensity factors, J-integral and the values of crack opening, hence, they do not influence material's fracture parameters in the framework of Griffiths–Irwin, Cherepanov–Reiss fracture criteria, critical crack openings or their generalizations (Guz 1991, 2021; Guz et al. 2020).

In the situations when initial stresses are significantly larger as compared to additional (operational) stresses, for investigating problems of such kind, in Guz (1980, 1991) the applicability of the approach within the linearized mechanics of deformable solid bodies (Guz 1999) was justified, while in Guz (1982, 1991) energy- and force-based criteria of brittle fracture of materials with initial (residual) stresses

V. Bogdanov (✉) · A. Guz · V. Nazarenko
S.P. Timoshenko Institute of Mechanics, National Academy of Science of Ukraine, Kyiv, Ukraine
e-mail: bogdanov@nas.gov.ua

A. Guz
e-mail: guz@nas.gov.ua

V. Nazarenko
e-mail: vmnazarenko@nas.gov.ua

© The Author(s), under exclusive license to Springer Nature Switzerland AG 2023

A. N. Guz et al. (eds.), *Advances in Mechanics*, Advanced Structured Materials 191,
https://doi.org/10.1007/978-3-031-37313-8_4

were formulated. The results of studying some problems of the fracture mechanics of materials with initial (residual) stresses, which were obtained with reliance on this approach, were presented in Bogdanov (2007, 2010, 2012), Bogdanov et al. (2015), Guz (1991, 2021).

Another group of non-classical problems of fracture mechanics is the fracture of bodies compressed along the parallel cracks they contain, when fracturing process is initiated by the local loss of stability in the part of material adjacent to the crack (Bolotin 1994, 2001; Guz et al. 1992, 2020; Kachanov 1988; Kienzler and Herrmann 2000; Wu 1979). Under such loading mode, singular parts in corresponding exact solutions of the problems of linear theory of elasticity are absent and, hence, all stress intensity factors are equal to zero, due to which classical fracture criteria are not applicable (Guz 2021; Guz et al. 2020). Many engineering problems related to the calculations of products with predetermined defects are reduced to the force-based scheme of compression along crack-like defects. Problems of this kind are rather typical in modeling the action of tectonic forces in mountainous terrain (model of fissured-layered massif), in calculating various supports, and in evaluating the strength and durability of concrete structure members. Various approaches to determining critical compression parameters, which correspond to the abovementioned local loss of stability, were analyzed in detail in Guz (2021), Guz et al. (2020). The results of investigating some problems on body compression along both isolated and interacting cracks with the use of the approach in the framework of the three-dimensional linearized theory of stability of deformable bodies are presented in Bogdanov and Nazarenko (1994), Guz (2014, 2021), and Guz et al. (1992, 2020).

It should be noted that although in terms of research subject the problems on the fracture of pre-stressed bodies under the action of initial stresses along cracks and the problem on the compression of materials along cracks are different, in the formulation of those problems there is an essential common point, viz., the presence of load components directed in parallel to cracks, whose influence, in fact, cannot be taken into account with the methods of classical fracture mechanics. This permits the two abovementioned groups of non-classical problems of fracture mechanics to be united and considered as problems of materials fracture under the action of forces directed along cracks. As it will be shown below, they can be investigated jointly, using the methodology based on relations of linearized mechanics of deformable solid bodies.

4.2 Approach to Studying the Problems

Below, brief information about the procedure used to investigate problems on the fracture of cracked bodies under the action of loads directed along cracks, and about the general formulation of corresponding boundary value problems is given.

As noted above, starting with the works (Guz 1980, 1991), to investigate problems of fracture mechanics for pre-stressed materials, when initial stresses act along the cracks the material contains and these initial stresses are significantly larger than operational stresses, an approach within the linearized mechanics of deformable solid

bodies started to be applied consistently. The key factor in substantiating this method is that the application of linearized relations for investigating the abovementioned class of fracture mechanics problems, on the one hand, permits broad use of the advantages of the linear model of the deformable body and, on the other, qualitative and quantitative description (as opposed to the classical procedures) of the main phenomenon related to the influence of the stress components acting along crack surfaces on fracture parameters.

In Guz (1981), Guz et al. (1992), Wu (1979), it was shown that under compression of bodies along parallel cracks they contain, the beginning (start) of the fracture process is caused by the loss of material's stability in local areas near the cracks, when compressive forces achieve the values critical for the given material and the geometry of cracks location. Here, to determine the critical values of the compressive forces mentioned, the relations of the three-dimensional linearized theory of deformable bodies stability (Guz 1999) can be used, since with the involvement of the abovementioned criterion of the fracture process beginning (start), the possibility of the transition of a part of the material in the vicinity of cracks into adjacent forms of equilibrium under small (as compared to the main values of the initial states) perturbations of stresses and displacements is analyzed.

It should be noted that until recently the abovementioned two classes of fracture mechanics problems, viz., the problems on the fracture of materials with initial stresses acting along cracks and the problems on the fracture of bodies under compression along cracks were considered separately, but at the same time, taking into account that there are common features in the formulations of and approaches to these two classes of problems, namely, the presence of the load component acting along the cracks and the use of linearized relations for problems solving, in Bogdanov et al. (2017), Guz et al. (2013), the applicability of the unified approach within the linearized mechanics of deformable solid bodies was substantiated for investigating fracture mechanics problems on pre-stressed cracked materials and the problems on the fracture of bodies compressed along cracks (the information about this method can also be found in Guz et al. (2020)).

This approach is simpler and more effective for determining critical (limit) loading parameters in the problems on bodies compression along the cracks they contain, since there is no need of individual investigations of eigenvalue problems within the 3D linearized theory of stability. The parameters mentioned are calculated in solving corresponding boundary value problems of the mechanics of fracture of pre-stressed materials, when under the continuous change of loading parameters, we determine the initial compressive stresses which, when achieved, lead to a resonance change in the amplitude values (of stresses and displacements) near crack tips. The initial loading parameters determined in this way will correspond to the eigenvalues of corresponding eigenvalue problems on bodies compression along cracks.

Besides, an important positive feature of this approach is the possibility to conduct investigations in a single general form for compressible and incompressible isotropic or transverse isotropic elastic bodies with arbitrary structures of elastic potential as applied to the theory of finite (large) initial strains, as well as various variants of the theory of small initial strains. There, the specification of material's model (e.g., the

use of elastic potential of one type or another) is only carried out at the final stage of the investigation—in the numerical analysis of the characteristic equations, the resolving integral equations, etc., obtained in the general form. It should also be noted that when considering composite materials in this work, it is assumed that crack sizes are significantly larger than the sizes of composite's structural elements, while the cases of cracks location in the interfaces of composite's components are not considered. With such assumptions, following, e.g., Broutman and Krock (1974), Dvorak (2000), Malmeister et al. (1980), we will use the continuum model of the composite with the reduced (averaged) characteristics of the transverse isotropic body.

Now, we present the principal relations of the linearized mechanics of deformable solid bodies, which will be used for solving particular problems. Figure 4.1 shows schematically an unbounded body with tensile or compressive initial (residual) stresses S_{11}^0 acting along cracks located in parallel planes $y_3 = \text{const}$. It should be noted that to carry out the investigation of the stress-strain state of pre-stressed bodies is more convenient in the Lagrangian coordinates y_j $(j = 1, 2, 3)$, which are related to the initial state caused by initial stresses S_{11}^0. These coordinates can be presented via the Cartesian coordinates of the non-deformed (natural) state of the body x_j $(j = 1, 2, 3)$ by the following relations

$$y_j = \lambda_j x_j, \quad j = 1, 2, 3, \tag{4.1}$$

where $\lambda_j = \text{const}$ are coefficients of elongation (contraction) along coordinate axes Oy_j, which are caused by initial stresses S_{11}^0. Besides, operational stresses (additional to the initial ones) also act on the body (normal stresses Q'_{33} are shown as an example).

Under the action of initial (residual) stresses S_{11}^0 only, a homogeneous stress-strain state emerges in the material (both isotropic and transverse isotropic). (It is assumed for transverse isotropic material that cracks are located in the planes of material's properties symmetry and, thus, initial stresses are directed along the sym-

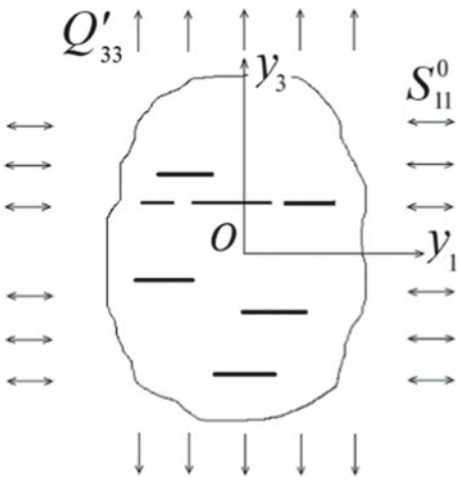

Fig. 4.1 Cracked body with initial stresses

metry axes of material's properties.) This stress-strain state is characterized by such expressions for components of the tensor of initial stresses $\tilde{S}^0$ and the vector of initial displacements $\mathbf{u}^0$:

$$S_{11}^0 = \text{const}, \ S_{22}^0 = \text{const}, \ S_{33}^0 = 0, \ S_{ij}^0 = 0, \ i \neq j; \ u_j^0 = \lambda_j^{-1} \left(\lambda_j - 1\right) y_j. \tag{4.2}$$

For compressible bodies, linearized equilibrium equations in displacements are of the form Bogdanov et al. (2017), Guz (1999), Guz et al. (2020)

$$\omega'_{ij\alpha\beta} \frac{\partial^2 u_\alpha}{\partial y_i \partial y_\beta} = 0, \tag{4.3}$$

where u_α are displacements caused by the action of initial and operational stresses. Boundary conditions in stresses on a part of S_1 surface are presented as

$$N_i^0 Q'_{ij} = P'_j, \tag{4.4}$$

where N_i^0 are components of the ort of the normal to the surface of the body in the initial state (the body state caused by initial stresses S_{11}^0), while boundary conditions in displacements on a part of S_2 surface are of the form

$$u_j = f'_j. \tag{4.5}$$

The components of the fourth rank elasticity tensor $\tilde{\omega}'$, which are involved in (4.3) and in the linearized elasticity relations

$$Q'_{ij} = \omega'_{ij\alpha\beta} \frac{\partial u_\alpha}{\partial y_\beta}, \tag{4.6}$$

are given by expressions

$$\omega'_{ij\alpha\beta} = \frac{\lambda_i \lambda_j \lambda_\alpha \lambda_\beta}{\lambda_1 \lambda_2 \lambda_3} \left[\delta_{ij}\delta_{\alpha\beta} A_{i\beta} + \left(1 - \delta_{ij}\right)\left(\delta_{i\alpha}\delta_{j\beta} + \delta_{i\beta}\delta_{j\alpha}\right) G_{ij}\right] + \frac{\lambda_i \lambda_\beta}{\lambda_1 \lambda_2 \lambda_3} \delta_{i\beta}\delta_{j\alpha} S_{\beta\beta}^0, \tag{4.7}$$

where δ_{ij} is Kronecker symbol, A_{ij} are elasticity constants, G_{ij} are shear moduli, $S_{\beta\beta}^0$ are initial stresses, and λ_m are coefficients of elongation (contraction) along coordinate axes Oy_m, that is caused by these initial stresses.

The dependence between components of Piola–Kirchhoff non-symmetric stress tensor $\tilde{Q}'$ and Lagrange symmetric stress tensor $\tilde{S}$ is given by relations (Bogdanov et al. 2017; Guz 1999; Guz et al. 2020)

$$Q'_{ij} = \frac{\lambda_i \lambda_j}{\lambda_1 \lambda_2 \lambda_3} S_{ij} + \frac{\lambda_i}{\lambda_1 \lambda_2 \lambda_3} S_{in}^0 \frac{\partial u_j}{\partial y_n}.$$

Representations of the general solutions of linearized equilibrium equations (4.3) via harmonic potentials were constructed in Bogdanov et al. (2017), Guz (1999), Guz et al. (2020). By assuming that the axis of material's isotropy coincides with axis Oy_3 of the coordinate system, and conditions $\lambda_1 = \lambda_2 \neq \lambda_3$, $S_{11}^0 = S_{22}^0$, $S_{33}^0 = 0$ are satisfied, we have such representations of the general solutions for the circular cylindrical coordinate system (r, θ, y_3) obtained from the Cartesian one (Bogdanov et al. 2017; Guz 1999; Guz et al. 2020):

in the case of non-equal roots of the characteristic equation ($n_1 \neq n_2$)

$$\begin{aligned}
u_r &= \frac{\partial\,(\varphi_1+\varphi_2)}{\partial r} - \frac{1}{r}\frac{\partial \varphi_3}{\partial \theta},\\
u_\theta &= \frac{1}{r}\frac{\partial\,(\varphi_1+\varphi_2)}{\partial \theta} + \frac{\partial \varphi_3}{\partial r},\\
u_3 &= m_1 n_1^{-1/2}\frac{\partial \varphi_1}{\partial z_1} + m_2 n_2^{-1/2}\frac{\partial \varphi_2}{\partial z_2},\\
Q'_{33} &= C_{44}\left(d_1 l_1 \frac{\partial^2 \varphi_1}{\partial z_1^2} + d_2 l_2 \frac{\partial^2 \varphi_2}{\partial z_2^2}\right),\\
Q'_{3r} &= C_{44}\left(d_1 n_1^{-1/2}\frac{\partial^2 \varphi_1}{\partial r \partial z_1} + d_2 n_2^{-1/2}\frac{\partial^2 \varphi_2}{\partial r \partial z_2} - n_3^{-1/2}\frac{1}{r}\frac{\partial^2 \varphi_3}{\partial \theta \partial z_3}\right),\\
Q'_{3\theta} &= C_{44}\left(d_1 n_1^{-1/2}\frac{1}{r}\frac{\partial^2 \varphi_1}{\partial \theta \partial z_1} + d_2 n_2^{-1/2}\frac{1}{r}\frac{\partial^2 \varphi_2}{\partial \theta \partial z_2} + n_3^{-1/2}\frac{\partial^2 \varphi_3}{\partial r \partial z_3}\right),\\
z_j &= n_j^{-1/2} y_3, \quad j = 1, 2, 3;
\end{aligned} \tag{4.8}$$

in the case of equal roots of the characteristic equation ($n_1 = n_2$)

$$\begin{aligned}
u_r &= -\frac{\partial \varphi}{\partial r} - z_1\frac{\partial F}{\partial r} - \frac{1}{r}\frac{\partial \varphi_3}{\partial \theta},\\
u_\theta &= -\frac{1}{r}\frac{\partial \varphi}{\partial \theta} - z_1\frac{1}{r}\frac{\partial F}{\partial \theta} + \frac{\partial \varphi_3}{\partial r},\\
u_3 &= (m_1 - m_2 + 1)\, n_1^{-1/2} F - m_1 n_1^{-1/2}\Phi - m_1 n_1^{-1/2} z_1 \frac{\partial F}{\partial z_1},\\
Q'_{33} &= C_{44}\left[(d_1 l_1 - d_2 l_2)\frac{\partial F}{\partial z_1} - d_1 l_1 \frac{\partial \Phi}{\partial z_1} - d_1 l_1 z_1 \frac{\partial^2 F}{\partial z_1^2}\right], \quad \Phi \equiv \frac{\partial \varphi}{\partial z_1},\\
Q'_{3r} &= C_{44}\left\{n_1^{-1/2}\frac{\partial}{\partial r}\left[(d_1 - d_2)\, F - d_1 \Phi\right]\right.\\
&\qquad \left. -\ n_1^{-1/2} d_1 z_1 \frac{\partial^2 F}{\partial r \partial z_1} - n_3^{-1/2}\frac{1}{r}\frac{\partial^2 \varphi_3}{\partial \theta \partial z_3}\right\},\\
Q'_{3\theta} &= C_{44}\left\{n_1^{-1/2}\frac{1}{r}\frac{\partial}{\partial \theta}\left[(d_1 - d_2)\, F - d_1 \Phi\right]\right.\\
&\qquad \left. -\ n_1^{-1/2} d_1 z_1 \frac{1}{r}\frac{\partial^2 F}{\partial \theta \partial z_1} + n_3^{-1/2}\frac{\partial^2 \varphi_3}{\partial r \partial z_3}\right\},
\end{aligned} \tag{4.9}$$

where the roots of the characteristic equations take the form

$$\begin{aligned}
n_{1,2} &= c' \pm \sqrt{c'^2 - \frac{\omega'_{3333}\omega'_{3113}}{\omega'_{1111}\omega'_{1331}}}, \quad n_3 = \frac{\omega'_{3113}}{\omega'_{1221}},\\
c' &= \frac{\omega'_{1111}\omega'_{3333} + \omega'_{3113}\omega'_{1331} - \left(\omega'_{1133} + \omega'_{1313}\right)^2}{2\omega'_{1111}\omega'_{1331}}.
\end{aligned} \tag{4.10}$$

In (4.8) and (4.9), the potentials $\varphi_j\left(r,\theta,z_j\right)$, $\varphi\left(r,\theta,z_j\right)$, and $F\left(r,\theta,z_j\right)$ $(j=1,2,3)$ satisfy Laplace's equations; the values C_{44}, m_i, d_i, and l_i $(i=1,2)$ are determined by the choice of material's model and are linked with components of elasticity tensor $\tilde{\omega}'$ (4.7) (Bogdanov et al. 2017; Guz 1999; Guz et al. 2020).
in the case of non-equal roots of the characteristic equation $(n_1 \neq n_2)$

$$C_{44}=\omega'_{1313},\quad m_i=\frac{\omega'_{1111}n_i-\omega'_{3113}}{\omega'_{1133}+\omega'_{1313}},\quad d_i=1+m_i,$$
$$l_i=\frac{\omega'_{3333}m_i-\omega'_{1133}n_i}{n_i d_i \omega'_{1313}},\quad i=1,2; \tag{4.11}$$

in the case of equal roots of the characteristic equation $(n_1=n_2)$ parameters C_{44}, m_1, d_1, d_2, l_1 are determined from (4.11), and parameters m_2, l_2 take the from

$$m_2=\frac{\omega'_{1133}-\omega'_{1313}}{\omega'_{1133}+\omega'_{1313}},\quad l_2=\frac{\omega'_{3333}(m_1+m_2-1)-\omega'_{1133}n_1}{n_1 d_2 \omega'_{1313}}. \tag{4.12}$$

In the case of axisymmetric linearized problems, the potential function f_3 in (4.8) and (4.9) should be set equal to zero, while the potential functions φ_1, φ_2 , φ, F are to be considered independent of coordinate θ.

Taking into account representations (4.8) and (4.9), the general statement of linearized problems (4.3)–(4.5) can be re-formulated in terms of harmonic potential functions $\varphi_j\left(r,\theta,z_j\right)$, $j=1,2,3$ (in the case of non-equal roots) and $\varphi\,(r,\theta,z_1)$, $F\,(r,\theta,z_1)$, $\varphi_3\,(r,\theta,z_3)$ (in the case of equal roots). For the spatial boundary value problems on pre-stressed bodies containing circular cracks (which are also referred to as penny-shaped cracks), considered in this work, we will present the potential functions mentioned as Henkel integral transform in radial coordinate, reduce the problems to paired (dual) integral equations and then to Fredholm integral equations of the second kind, which will be investigated numerically.

4.3 Formulation of the Problems

Consider spatial problems on pre-stressed half-bounded body with a near-surface circular crack and those on an unbounded body with initial (residual) stresses, containing two parallel coaxial circular cracks. It should be noted that the former geometric scheme permits the analysis of the influence of initial stresses as well as the effect of the interaction of cracks and the free surface of the body on stress intensity factors in the vicinity of crack contours and on the critical compression parameters, which, when achieved, lead to the local loss of material's stability near cracks. The latter geometric scheme permits the evaluation of the influence of parallel cracks interaction on those parameters.

4.3.1 Initially Stressed Half-Space with a Near-Surface Circular Crack

Consider an elastic body occupying half-space $y_3 \geqslant -h$. There are initial stresses $S_{11}^0 = S_{22}^0$ acting along a near-surface crack of radius $r = a$, located in $y_3 = 0$ plane centered on axis Oy_3: $\{0 \leqslant r \leqslant a, 0 \leqslant \theta < 2\pi, y_3 = 0\}$ (Fig. 4.2). We assume that additional (with respect to initial stresses) fields of normal and shear forces Q'_{33} and Q'_{3r} act on crack faces, while the half-space boundary is free of loads. Boundary conditions of such non-axisymmetric problem are of the form

$$\begin{gathered} Q'_{33} = -\sigma(r,\theta),\ Q'_{3r} = -\tau_r(r,\theta),\ Q'_{3\theta} = 0\ (y_3 = (0)_{\pm},\ 0 \leqslant r \leqslant a), \\ Q'_{33} = 0,\quad Q'_{3r} = 0,\quad Q'_{3\theta} = 0\quad (y_3 = -h,\ 0 \leqslant r < \infty). \end{gathered} \tag{4.13}$$

(Here and further $0 \leqslant \theta < 2\pi$, and subscripts "+" and "–" denote the upper and lower crack faces respectively).

Besides, the conditions of the attenuation of displacement vector and stress tensor components at infinity must be satisfied as

$$u_j \to 0,\quad Q'_{ij} \to 0\quad (r \to +\infty,\ y_3 \to +\infty). \tag{4.14}$$

Further, in constructing the solution of the problem examined, it is convenient to divide the half-space $y_3 \geqslant -h$ into two domains: domain "1" is the half-space $y_3 \geqslant 0$ and domain "2" is the layer $-h \leqslant y_3 \leqslant 0$. All the values relating to each of these domains will be marked with superscripts "(1)" and "(2)". For such subdivision into two domains, on the domain boundary (when $y_3 = 0$) outside the crack, it is necessary that the conditions of continuity for displacement and stress vectors be satisfied. Then the boundary conditions (4.13) can be written as

$$\begin{gathered} Q'^{(2)}_{33} = -\sigma(r,\theta),\ Q'^{(2)}_{3r} = -\tau_r(r,\theta),\ Q'^{(2)}_{3\theta} = 0\ (y_3 = 0,\ 0 \leqslant r \leqslant a), \\ Q'^{(2)}_{33} = 0,\ Q'^{(2)}_{3r} = 0,\ Q'^{(2)}_{3\theta} = 0\ (y_3 = -h,\ 0 \leqslant r < \infty), \\ u_3^{(1)} = u_3^{(2)},\ u_r^{(1)} = u_r^{(2)},\ u_\theta^{(1)} = u_\theta^{(2)}\ (y_3 = 0,\ a < r < \infty), \\ Q'^{(1)}_{33} = Q'^{(2)}_{33},\ Q'^{(1)}_{3r} = Q'^{(2)}_{3r},\ Q'^{(1)}_{3\theta} = Q'^{(2)}_{3\theta}\ (y_3 = 0,\ 0 \leqslant r < \infty). \end{gathered} \tag{4.15}$$

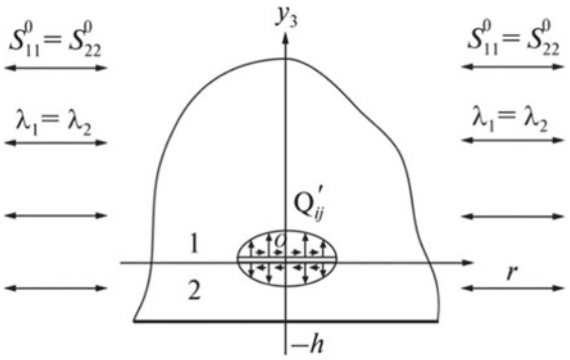

Fig. 4.2 Pre-stressed semi-infinite body with a circular near-surface crack

By using the representations of general solutions in terms of potential harmonic functions of form (4.8) for non-equal roots and form (4.9) for equal roots, from (4.15) we obtain the problem formulation in terms of harmonic potential functions $\varphi_i^{(k)}(r, \theta, z_j)$, $k = 1, 2$, $i, j = 1, 2, 3$ (in the case of non-equal roots) and $\varphi^{(k)}(r, \theta, z_1)$, $F^{(k)}(r, \theta, z_1)$ and $\varphi_3^{(k)}(r, \theta, z_3)$, $k = 1, 2$ (in the case of equal roots).

The formulations of axisymmetric problems for the pre-stressed half-space with mode I, mode II, or mode III cracks are carried out in the similar way, if in the corresponding boundary conditions, it is set that $u_\theta^{(k)} = 0$, $Q'^{(k)}_{3\theta} = 0$, $k = 1, 2$, while other components of displacement vector and stress tensor are considered to be independent of angular component θ.

4.3.2 Pre-stressed Body with Two Parallel Circular Cracks

Consider an unbounded elastic body with initial stresses $S^0_{11} = S^0_{22}$ that contains two circular cracks of the same radius $r = a$, which are located in parallel planes $y_3 = 0$ and $y_3 = -2h$ with centers on the Oy_3 axis (Fig. 4.3). Additional stresses Q'_{33} and Q'_{3r} (with respect to the initial ones $S^0_{11} = S^0_{22}$) acting on crack faces and the boundary condition are

$$\begin{aligned} &Q'_{33} = -\sigma(r, \theta),\ Q'_{3r} = -\tau_r(r, \theta),\ Q'_{3\theta} = 0\ (y_3 = (0)_\pm,\ 0 \leqslant r \leqslant a), \\ &Q'_{33} = -\sigma(r, \theta),\ Q'_{3r} = -\tau_r(r, \theta),\ Q'_{3\theta} = 0\ (y_3 = (-2h)_\pm,\ 0 \leqslant r \leqslant a), \end{aligned} \tag{4.16}$$

where $0 \leqslant \theta < 2\pi$, and subscripts "+" and "–" denote the upper and lower cracks faces respectively.

For the case considered, the symmetry of the geometric and force-based schemes of the problem in respect of plane $y_3 = -h$ exists. Due to that, given (4.16), it can be re-formulated as a mathematically equivalent problem on the half-space $y_3 \geqslant -h$

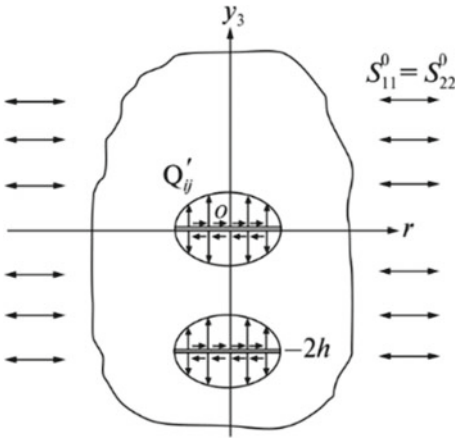

Fig. 4.3 Pre-stressed body with two parallel coaxial circular cracks

with a single mode I or mode II crack located in the plane $y_3 = 0$, with the following boundary conditions on its faces and on the half-space boundary:

for *mode I crack*

$$\begin{gathered} Q'_{33} = -\sigma(r,\theta), \quad Q'_{3r} = 0, \quad Q'_{3\theta} = 0 \quad (y_3 = (0)_{\pm},\ 0 \leqslant r \leqslant a), \\ u_3 = 0, \quad Q'_{3r} = 0, \quad Q'_{3\theta} = 0 \quad (y_3 = -h,\ 0 \leqslant r \leqslant a); \end{gathered} \tag{4.17}$$

for *mode II crack*

$$\begin{gathered} Q'_{33} = 0, \quad Q'_{3r} = -\tau_r(r,\theta), \quad Q'_{3\theta} = 0 \quad (y_3 = (0)_{\pm},\ 0 \leqslant r \leqslant a), \\ u_r = 0, \quad u_\theta = 0, \quad Q'_{33} = 0 \quad (y_3 = -h,\ 0 \leqslant r \leqslant a). \end{gathered} \tag{4.18}$$

Besides, the conditions of the attenuation of the displacement vector and stress tensor components at infinity (4.14) must be satisfied.

As can be seen from (4.17) and (4.18), the formulation of the problem on a space with two parallel coaxial cracks (4.16) is mathematically equivalent to the problems on the half-space $y_3 \geqslant -h$ with a mode I crack or a mode II crack that is parallel to its surface when the half-space boundary rests on a smooth rigid foundation.

We will confine ourselves to the axisymmetric problem and will consider individually the cases when normal stresses Q'_{33} (mode I cracks), radial shear stresses Q'_{3r} (mode II cracks) or tangential torsional stresses $Q'_{3\theta}$ (mode III cracks) act on crack faces.

Mode I cracks. Taking into account the symmetry of the geometric and force-based schemes of the problem in respect of plane $y_3 = -h$, we have the following boundary conditions specified on the cracks faces and on the half-space boundary and crack faces

$$\begin{gathered} Q'_{33} = -\sigma(r), \quad Q'_{3r} = 0 \quad (y_3 = (0)_{\pm},\ 0 \leqslant r \leqslant a), \\ u_3 = 0, \quad Q'_{3r} = 0 \quad (y_3 = -h,\ 0 \leqslant r \leqslant \infty). \end{gathered} \tag{4.19}$$

The half-space $y_3 \geqslant -h$ is conditionally divided into two domains: "1"—the half-space $y_3 \geqslant 0$ and "2"—the layer $-h \leqslant y_3 \leqslant 0$. All the values relating to each of the domains mentioned are marked by superscripts "(1)" and "(2)". Taking into account the conditions of the continuity of stresses and displacements on the boundaries of the domains, new boundary conditions of the problem are obtained from (4.17)

$$\begin{gathered} Q'^{(2)}_{33} = -\sigma(r),\ Q'^{(2)}_{3r} = 0 \quad (y_3 = 0,\ 0 \leqslant r \leqslant a), \\ u^{(2)}_3 = 0,\ Q'^{(2)}_{3r} = 0 \quad (y_3 = -h,\ 0 \leqslant r \leqslant \infty), \\ u^{(1)}_3 = u^{(2)}_3,\ u^{(1)}_r = u^{(2)}_r \quad (y_3 = 0,\ a < r < \infty), \\ Q'^{(1)}_{33} = Q'^{(2)}_{33},\ Q'^{(1)}_{3r} = Q'^{(2)}_{3r} \quad (y_3 = 0,\ 0 \leqslant r < \infty). \end{gathered} \tag{4.20}$$

Mode II cracks. The tangential radial stresses of the intensity $t_r(r)$ are applied to crack faces antisymmetrically in respect of the planes of cracks location. Taking into account the symmetry of the geometric and force-based schemes of the problem with respect to the plane $y_3 = -h$, equidistant from the cracks and dividing the half-space

$y_3 \geqslant -h$ into two parts, namely, the half-space $y_3 \geqslant 0$ (domain "1") and the layer $-h \leqslant y_3 \leqslant 0$ (domain "2"), we have such boundary conditions of the problem on mode II cracks:

$$\begin{gathered} Q_{33}^{\prime(2)} = 0,\ Q_{3r}^{\prime(2)} = -\tau_r(r) \quad (y_3 = 0,\ 0 \leqslant r \leqslant a), \\ u_r^{(2)} = 0,\ Q_{33}^{\prime(2)} = 0 \quad (y_3 = -h,\ 0 \leqslant r \leqslant \infty), \\ u_3^{(1)} = u_3^{(2)},\ u_r^{(1)} = u_r^{(2)} \quad (y_3 = 0,\ a < r < \infty), \\ Q_{33}^{\prime(1)} = Q_{33}^{\prime(2)},\ Q_{3r}^{\prime(1)} = Q_{3r}^{\prime(2)} \quad (y_3 = 0,\ 0 \leqslant r < \infty). \end{gathered} \tag{4.21}$$

By using the representations of general solutions for displacements and stresses via potential functions (4.8) (for non-equal real roots) and (4.9) (for equal roots), from boundary conditions (4.20) and (4.21) the formulations of problems for mode I crack and mode II crack are obtained in terms of potential functions ${\varphi_i}^{(k)}\left(r, z_j\right)$, $i, j, k = 1, 2$ (in the case of non-equal roots) and $\varphi^{(k)}(r, z_1)$, $F^{(k)}(r, z_1)$, $k = 1, 2$ (in the case of equal roots).

Mode III cracks. The tangential torsional stresses of the intensity $\tau_\theta(r)$ are applied to crack faces antisymmetrically in respect of cracks location planes. With this loading scheme, only the components of displacement vector u_θ and stress tensor $Q'_{3\theta}$ will be non-zero, and owing to the axisymmetric nature of the problem they do not depend on the angular coordinate θ. The boundary conditions of the problem on mode III cracks can be written as follows

$$\begin{gathered} Q_{3\theta}^{\prime(2)} = -\tau_\theta(r) \quad (y_3 = 0,\ 0 \leqslant r \leqslant a), \\ u_\theta^{(2)} = 0 \quad (y_3 = -h,\ 0 \leqslant r \leqslant \infty), \\ u_\theta^{(1)} = u_\theta^{(2)} \quad (y_3 = 0,\ a < r < \infty), \\ Q_{3\theta}^{\prime(1)} = Q_{3\theta}^{\prime(2)} \quad (y_3 = 0,\ 0 \leqslant r < \infty). \end{gathered} \tag{4.22}$$

The representations of general solutions in this case, given (4.8) and (4.9), are of the same form for the cases of both equal and non-equal roots, specifically

$$u_\theta = \frac{\partial}{\partial r}\varphi_3(r, z_3), \quad Q'_{3\theta} = C_{44} n_3^{-1/2} \frac{\partial^2}{\partial r \partial z_3}\varphi_3(r, z_3). \tag{4.23}$$

By using representations (4.23) we obtain the formulation of the problem for elastic body with mode III cracks in terms of the potential harmonic function $\varphi_3(r, z_3)$

$$\begin{aligned} C_{44} n_3^{-1/2} \frac{\partial^2 \varphi_3^{(2)}}{\partial r \partial z_3} &= -\tau_\theta(r) \quad (y_3 = 0,\ 0 \leqslant r \leqslant a), \\ \frac{\partial \varphi_3^{(2)}}{\partial r} &= 0 \quad (y_3 = -h,\ 0 \leqslant r < \infty), \\ \frac{\partial \varphi_3^{(1)}}{\partial r} &= \frac{\partial \varphi_3^{(2)}}{\partial r} \quad (y_3 = 0,\ a < r < \infty), \\ \frac{\partial^2 \varphi_3^{(1)}}{\partial r \partial z_3} &= \frac{\partial^2 \varphi_3^{(2)}}{\partial r \partial z_3} \quad (y_3 = 0,\ 0 \leqslant r < \infty). \end{aligned} \tag{4.24}$$

4.4 Fredholm Integral Equations

The mixed boundary value problems on harmonic potential functions, which were formulated in the previous section will be solved by first reducing them to paired (dual) integral equations and then—to systems of Fredholm integral equations of the second kind. For that, harmonic potentials will be represented via Fourier series (for non-axisymmetric problems) and Hankel integral expansions in radial coordinates. The process of solving non-axisymmetric problems will be exemplified by the problem on a half-space with a near-surface crack, and the solution of axisymmetric problems—by that on a body containing two parallel mode I cracks.

4.4.1 Half-Space with a Near-Surface Circular Crack

We will show calculation procedures for the case of equal roots of the characteristic equation ($n_1 = n_2$); the procedures for non-equal roots ($n_1 \neq n_2$) are carried out in the similar way.

The external loads on the crack faces (the right-hand parts of the first two expressions in (4.15)) are presented as Fourier series in coordinate θ, assuming that they are even functions in this coordinate

$$\sigma\,(r,\theta) = \sum_{n=0}^{\infty} \sigma^{(n)}(r)\cos n\theta\ , \quad \tau_r\,(r,\theta) = \sum_{n=0}^{\infty} \tau_r{}^{(n)}(r)\cos n\theta\ , \tag{4.25}$$

where coefficients in the expansions are of the form:

$$\begin{aligned}
\sigma^{(0)}\,(r) &= \frac{1}{\pi}\int_0^{\pi} \sigma\,(r,\theta)\,d\theta,\\
\tau_r^{(0)}\,(r) &= \frac{1}{\pi}\int_0^{\pi} \tau_r\,(r,\theta)\,d\theta,\\
\sigma^{(n)}\,(r) &= \frac{2}{\pi}\int_0^{\pi} \sigma\,(r,\theta)\cos n\theta\ d\theta,\\
\tau_r^{(n)}\,(r) &= \frac{2}{\pi}\int_0^{\pi} \tau_r\,(r,\theta)\cos n\theta\ d\theta, \quad n = 1, 2, \ldots.
\end{aligned} \tag{4.26}$$

In the case when $\sigma\,(r,\theta)$ and $\tau_r\,(r,\theta)$ are odd functions in θ, their transforms into Fourier series will be similar if cosines are changed to sines in (4.25); in the general case, when loads are arbitrary functions, the superposition of solutions should be used.

We present potential functions $\varphi^{(k)}\,(r,\theta,z_1)$, $F^{(k)}\,(r,\theta,z_1)$ and $\varphi_3^{(k)}\,(r,\theta,z_3)$ $(k = 1, 2)$ as Fourier series in coordinate θ with coefficients in the form of Hankel integral equations in radial coordinate r of the order corresponding to the harmonic in θ

$$
\begin{aligned}
\varphi^{(1)}(r,\theta,z_1) &= -\sum_{n=0}^{\infty}\cos n\theta\int_0^{\infty} B_n(\lambda)e^{-\lambda z_1}J_n(\lambda r)\frac{d\lambda}{\lambda},\\
F^{(1)}(r,\theta,z_1) &= \sum_{n=0}^{\infty}\cos n\theta\int_0^{\infty} A_n(\lambda)e^{-\lambda z_1}J_n(\lambda r)d\lambda,\\
\varphi_3^{(1)}(r,\theta,z_3) &= \sum_{n=1}^{\infty}\sin n\theta\int_0^{\infty} C_n(\lambda)e^{-\lambda z_3}J_n(\lambda r)\frac{d\lambda}{\lambda},\\
\varphi^{(2)}(r,\theta,z_1) &= \sum_{n=0}^{\infty}\cos n\theta\int_0^{\infty}\left[B_n^{(1)}(\lambda)\sinh\lambda(h_1+z_1)\right.\\
&\quad\left.+\ B_n^{(2)}(\lambda)\cosh\lambda(h_1+z_1)\right]J_n(\lambda r)\frac{d\lambda}{\lambda\sinh\lambda h_1},\\
F^{(2)}(r,\theta,z_1) &= \sum_{n=0}^{\infty}\cos n\theta\int_0^{\infty}\left[A_n^{(1)}(\lambda)\cosh\lambda(h_1+z_1)\right.\\
&\quad\left.+\ B_n^{(2)}(\lambda)\sinh\lambda(h_1+z_1)\right]J_n(\lambda r)\frac{d\lambda}{\sinh\lambda h_1},\\
\varphi_3^{(2)}(r,\theta,z_3) &= \sum_{n=1}^{\infty}\sin n\theta\int_0^{\infty}\left[C_n^{(1)}(\lambda)\cosh\lambda(h_3+z_3)\right.\\
&\quad\left.+\ C_n^{(2)}(\lambda)\sinh\lambda(h_3+z_3)\right]J_n(\lambda r)\frac{d\lambda}{\lambda\sinh\lambda h_3},\\
&\qquad h_j = n_j^{-1/2}h,\quad j=1,3.
\end{aligned}
\tag{4.27}
$$

In expressions (4.27), A_n, B_n, C_n, $A_n^{(k)}$, $B_n^{(k)}$, and $C_n^{(k)}$ $(k=1,2)$ are unknown functions that are to be determined. It should be noted that the presentation of potential functions as (4.27) ensures that conditions (4.14) are satisfied.

Substitute expressions (4.26) and (4.27) into boundary conditions (4.15). Then, from the conditions presented in the second and fourth lines of (4.15), which are set on all planes $y_3=-h$, $y_3=0$, we obtain six relations linking nine functions A_n, B_n, C_n, $A_n{}^{(i)}$, $B_n^{(i)}$, and $C_n^{(i)}$ $(i=1,2)$

$$
\begin{aligned}
B_n^{(1)}(\lambda) &= \mu_1 A_n^{(2)}(\lambda) + \left(1 - \frac{d_2}{d_1}\right) A_n^{(1)}(\lambda),\\
B_n^{(2)}(\lambda) &= \mu_1 A_n^{(1)}(\lambda) + \left(1 - \frac{d_2 l_2}{d_1 l_1}\right) A_n^{(2)}(\lambda), \quad C_n^{(2)}(\lambda) = 0,\\
A_n(\lambda) = &\left[\frac{\mu_1}{k}(1 + \coth\mu_1) - 1\right] A_n^{(1)}(\lambda)\\
&+ \left[\frac{\mu_1}{k}(1 + \coth\mu_1) + 1\right] A_n^{(2)}(\lambda),\\
B_n(\lambda) = &\left[\left(1 - \frac{d_2 l_2}{d_1 l_1}\right)\frac{\mu_1}{k}(1 + \coth\mu_1)\right.\\
&\left. - \left(1 - \frac{d_2}{d_1}\right) - \mu_1 \coth\mu_1\right] A_n^{(1)}(\lambda)\\
&+ \left[\left(1 - \frac{d_2 l_2}{d_1 l_1}\right)\frac{\mu_1}{k}(1 + \coth\mu_1)\right.\\
&\left. + \left(1 - \frac{d_2 l_2}{d_1 l_1}\right) - \mu_1\right] A_n^{(2)}(\lambda),\\
C_n(\lambda) &= -C_n^{(1)}(\lambda), \quad \mu_1 = \lambda h_1, \quad k = \frac{d_2(l_1 - l_2)}{d_1 l_1}.
\end{aligned}
\tag{4.28}
$$

From the remaining boundary conditions (the first and the third lines in (4.15)), taking into account the following relations (Watson 1995)

$$
\begin{aligned}
\frac{2n}{\lambda r} J_n(\lambda r) &= J_{n-1}(\lambda r) + J_{n+1}(\lambda r),\\
2\frac{\partial J_n(\lambda r)}{\partial(\lambda r)} &= J_{n-1}(\lambda r) - J_{n+1}(\lambda r),
\end{aligned}
$$

and equating to zero the relations at $\cos n\theta$, $\sin n\theta$, we obtain (individually for each nth harmonic in coordinate θ) the system of paired integral equations

$$
\begin{aligned}
&\int_0^\infty \left\{n_1^{-1/2} d_1 \left[\mu_1 A_n^{(1)} + (k + \mu_1 \coth\mu_1) A_n^{(2)}\right] - n_3^{-1/2} C_n^{(1)}\right\}\\
&\qquad \times J_{n+1}(\lambda r)\lambda d\lambda = -\frac{1}{C_{44}}\left[\tau_r^{(n)}(r) + \tau_\theta^{(n)}(r)\right], \quad r \leqslant a,\\
&\int_0^\infty \left\{n_1^{-1/2} d_1 \left[\mu_1 A_n^{(1)} + (k + \mu_1 \coth\mu_1) A_n^{(2)}\right] + n_3^{-1/2} C_n^{(1)}\right\}\\
&\qquad \times J_{n-1}(\lambda r)\lambda d\lambda = \frac{1}{C_{44}}\left[\tau_r^{(n)}(r) - \tau_\theta^{(n)}(r)\right], \quad r \leqslant a,\\
&\int_0^\infty \left[(k - \mu_1 \coth_1) A_n^{(1)} - \mu_1 A_n^{(2)}\right] J_n(\lambda r)\lambda d\lambda\\
&\qquad = -\frac{\sigma^{(n)}(r)}{C_{44} d_1 l_1}, \quad r \leqslant a,
\end{aligned}
\tag{4.29}
$$

$$
\begin{aligned}
&\int_0^\infty X_1 J_{n+1}(\lambda r)\, d\lambda = 0, \quad r > a,\\
&\int_0^\infty X_2 J_{n-1}(\lambda r)\, d\lambda = 0, \quad r > a,\\
&\int_0^\infty X_3 J_n(\lambda r)\, d\lambda = 0, \quad r > a,
\end{aligned}
$$

where the following notations are used

$$
\begin{aligned}
X_1 = &\left(1-\frac{d_2 l_2}{d_1 l_1}\right)(1+\coth\mu_1)\left[\frac{\mu_1}{k}A_n^{(1)}+\left(1+\frac{\mu_1}{k}\right)A_n^{(2)}\right] \\
&- C_n^{(1)}(1+\coth\mu_3)\,, \\
X_2 = &\left(1-\frac{d_2 l_2}{d_1 l_1}\right)(1+\coth\mu_1)\left[\frac{\mu_1}{k}A_n^{(1)}+\left(1+\frac{\mu_1}{k}\right)A_n^{(2)}\right] \\
&+ C_n^{(1)}(1+\coth\mu_3)\,, \\
X_3 = &\,2\left(1-\frac{d_2 l_2}{d_1 l_1}\right)\left[\left(1-\frac{\mu_1}{k}\right)A_n^{(1)}-\frac{\mu_1}{k}A_n^{(2)}\right](1+\coth\mu_1)\,.
\end{aligned}
\tag{4.30}
$$

To solve the system of paired equations (4.29), in accordance with the substitution method (Uflyand 1977), we present X_1, X_2, and X_3, given by (4.30) in the form that provides the identical satisfaction of those parts of the system of paired equations which are specified in the range $r > a$. Now, we introduce new unknown functions $\varphi(t)$, $\psi(t)$, and $\omega(t)$, which are continuous along with their first derivatives in the segment $[0, a]$, and represent via these functions the expressions X_j $(j = 1, 2, 3)$ as

$$
\begin{aligned}
X_1 &= \sqrt{\frac{\pi}{2}}\lambda^{3/2}\int_0^a \sqrt{t}\varphi(t)\,J_{n+1/2}(\lambda t)\,dt \\
&= \sqrt{\frac{\pi\lambda}{2}}\int_0^a \tilde{\varphi}(t)\left[a^{-n+1/2}J_{n-1/2}(\lambda a)-t^{-n+1/2}J_{n-1/2}(\lambda t)\right]dt, \\
X_2 &= \sqrt{\frac{\pi\lambda}{2}}\int_0^a \sqrt{t}\psi(t)J_{n-1/2}(\lambda t)dt, \\
X_3 &= \sqrt{\frac{\pi\lambda}{2}}\int_0^a \sqrt{t}\omega(t)J_{n+1/2}(\lambda t)dt \\
&= \sqrt{\frac{\pi}{2\lambda}}\int_0^a \tilde{\omega}(t)\left[a^{-n+1/2}J_{n-1/2}(\lambda a)-t^{-n+1/2}J_{n-1/2}(\lambda t)\right]dt, \\
\tilde{\varphi}(t) &\equiv \frac{d}{dt}\left[t^n\varphi(t)\right], \quad \tilde{\omega}(t) \equiv \frac{d}{dt}\left[t^n\omega(t)\right].
\end{aligned}
\tag{4.31}
$$

By using Weber–Schafheitling discontinuous integral (Bateman and Erdelyi 1953)

$$
\int_0^\infty \sqrt{\lambda}J_{n+1/2}(\lambda a)\,J_n(\lambda t) = \begin{cases} 0, & 0 \leqslant a < t \\ \sqrt{\dfrac{2}{\pi}}\dfrac{t}{a^{n+1/2}\sqrt{a^2-t^2}}, & 0 < t < a \end{cases}
\tag{4.32}
$$

and differentiation formulas for Bessel functions (Watson 1995)

$$
t^{-n}\frac{d}{dt}\left[t^n J_n(\lambda t)\right] = \lambda J_{n-1}(\lambda t), \quad t^n\frac{d}{dt}\left[t^{-n}J_n(\lambda t)\right] = -\lambda J_{n+1}(\lambda t),
\tag{4.33}
$$

it can be shown that the three last equations in system (4.29) (for the range $r > a$) are satisfied identically. Then, from the remaining three equations in (4.29) (for the range

$r \leqslant a$) we obtain Fredholm integral equations of the second kind (the procedure is shown in more detail in Bogdanov et al. (2017)):

$$\begin{aligned}
&(sk+q)\, f_1(\xi) + (sk-q)\, f_2(\xi) + \frac{4}{\pi}\int_0^1 f_1(\eta)\, K_{11}(\xi,\eta)\, d\eta \\
&\quad + \frac{4}{\pi}\int_0^1 f_2(\eta)\, K_{12}(\xi,\eta)\, d\eta + \frac{4}{\pi}\int_0^1 f_3(\eta)\, K_{13}(\xi,\eta)\, d\eta \\
&\qquad = \frac{8\xi}{\pi}\int_0^{\pi/2} \nu_1'(\xi\sin\theta) d\theta, \quad 0 \leqslant \xi, \eta \leqslant 1, \\
&(sk-q)\, f_1(\xi) + (sk+q)\, f_2(\xi) + \frac{4}{\pi}\int_0^1 f_1(\eta)\, K_{21}(\xi,\eta)\, d\eta \\
&\quad + \frac{4}{\pi}\int_0^1 f_2(\eta)\, K_{12}(\xi,\eta)\, d\eta + \frac{4}{\pi}\int_0^1 f_3(\eta)\, K_{23}(\xi,\eta)\, d\eta \\
&\qquad = \frac{8\xi}{\pi}\int_0^{\pi/2} \nu_2'(\xi\sin\theta)\, d\theta, \quad 0 \leqslant \xi, \eta \leqslant 1, \\
&skf_3(\xi) + \frac{4}{\pi}\int_0^1 f_1(\eta)\, K_{31}(\xi,\eta)\, d\eta + \frac{4}{\pi}\int_0^1 f_2(\eta)\, K_{32}(\xi,\eta)\, d\eta \\
&\quad \frac{4}{\pi}\int_0^1 f_3(\eta)\, K_{33}(\xi,\eta)\, d\eta = -\frac{8\xi}{\pi}\int_0^{\pi/2} u'(\xi\sin\theta) d\theta, \\
&\qquad 0 \leqslant \xi, \eta \leqslant 1, \quad s = \frac{n_1^{-1/2} d_1^2 l_1}{d_1 l_1 - d_2 l_2}, \quad q = n_3^{-1/2}.
\end{aligned} \tag{4.34}$$

The following dimensionless variables and functions are introduced in (4.34):

$$\begin{aligned}
\xi &= \frac{x}{a}, \quad \eta = \frac{t}{a}, \quad \beta = \frac{h}{a}, \\
f_1(\xi) &= a^{-n-1}\tilde{\varphi}(x) \\
&= a^{-n-1}\frac{d}{dx}\left[x^n \varphi(x)\right], \\
f_2(\xi) &= a^{-n-1} x^n \psi(x), \\
f_3(\xi) &= a^{-n}\tilde{\omega}(x) \\
&= a^{-n}\frac{d}{dx}\left[x^n \omega(x)\right], \\
u(\xi) &= \frac{\xi^n}{C_{44} l_1 \sqrt{n_1}} \sigma^{(n)}(a\xi), \\
\nu_1(\xi) &= \frac{\xi^{2n}}{C_{44}} \int_0^{\xi} \rho^{-n} \tau_r^{(n)}(a\rho)\, d\rho, \\
\nu_2(\xi) &= \frac{1}{C_{44}} \int_0^{\xi} \rho^{n} \tau_r^{(n)}(a\rho)\, d\rho.
\end{aligned} \tag{4.35}$$

The kernels in (4.34) are of the form Bogdanov et al. (2017):

$$K_{22}(\xi,\eta) = 2skn\beta_1\xi^{n-1}\eta^{-n-1}S_n(z_{11}) + \frac{4s}{k}n\beta_1^3\xi^{n-2}\frac{\eta^{-n-2}}{z_{11}^2-1}$$
$$\times\left\{\left[\left(\frac{8}{z_{11}^2-1}+n(n-1)+6\right)\frac{4\beta_1^2}{\xi\eta}-6z_{11}\right]S_n(z_{11})\right.$$
$$\left.+(n-1)\left[3\left(z_{11}^2-1\right)+\frac{16\beta_1^2z_{11}}{\xi\eta}\right]P_n(z_{11})\right\}$$
$$-2sn\beta_1\xi^{n-2}\eta^{-n-2}\left[\left(\xi\eta-\frac{8\beta_1^2z_{11}}{z_{11}^2-1}\right)S_n(z_{11})+4\beta_1^2(n-1)P_n(z_{11})\right]$$
$$+2qn\beta_3\xi^{n-1}\eta^{-n-1}S_n(z_{13}), \qquad (4.36)$$

etc., where

$$\beta_j = \beta n_j^{-1/2} = \frac{h}{a}n_j^{-1/2} = \frac{h_j}{a}, \quad z_{1j} = \frac{4\beta_j^2+\xi^2+\eta^2}{2\xi\eta}, \quad j=1,3,$$
$$S_n(z) = \frac{Q_n(z)-zQ_{n-1}(z)}{4\left(z^2-1\right)}, \quad P_n(z) = \frac{Q_{n-1}(z)}{4\left(z^2-1\right)},$$

$Q_n(z)$ is Lagrange function of the second kind. The geometric parameter $\beta = ha^{-1}$ is the dimensionless distance from the crack to the boundary surface of the body.

In the similar way, axisymmetric problems on a semi-infinite body containing near-surface mode I, mode II, and mode III cracks can be reduced to Fredholm integral equations of the second kind (Bogdanov et al. 2017; Nazarenko et al. 2000).

So, for *the axisymmetric problem on mode I crack* in a semi-infinite pre-stressed body, when normal stresses of $\sigma(r)$ intensity act on crack faces, in the case of equal roots we obtain such system of Fredholm integral equations of the second kind

$$f(\xi)+\frac{4}{\pi k}\int_0^1 f(\eta)K_{11}(\xi,\eta)\,d\eta - \frac{4}{\pi k}\int_0^1 g(\eta)K_{12}(\xi,\eta)\,d\eta$$
$$= -\frac{4}{\pi k}\int_0^{\pi/2} s(\xi\sin\theta)\,d\theta,$$
$$g(\xi)+\frac{4}{\pi k}\int_0^1 f(\eta)K_{21}(\xi,\eta)\,d\eta - \frac{4}{\pi k}\int_0^1 g(\eta)K_{22}(\xi,\eta)\,d\eta = 0, \qquad (4.37)$$
$$s(\xi) = \frac{\xi}{C_{44}d_1l_1}\sigma(a\xi),$$

with the kernels

$$
\begin{aligned}
K_{11}(\xi,\eta) &= -\left[\frac{k}{2} I_1(2\beta_1,\eta) + \beta_1 I_2(2\beta_1,\eta) + \frac{\beta_1^2}{k} I_3(2\beta_1,\eta)\right],\\
K_{12}(\xi,\eta) &= \frac{\beta_1^2}{k}\left[\eta^{-1} I_2(2\beta_1,\eta) - I_2(2\beta_1,1)\right],\\
K_{21}(\xi,\eta) &= -\frac{\beta_1^2}{k}\xi I_4(2\beta_1,\eta),\\
K_{22}(\xi,\eta) &= \xi\left\{\frac{k}{2}\left[\eta^{-1} I_1(2\beta_1,\eta) - I_1(2\beta_1,1)\right]\right.\\
&\quad - \beta_1\left[\eta^{-1} I_2(2\beta_1,\eta)\, I_2(2\beta_1,1)\right]\\
&\quad \left. + \frac{\beta_1^2}{k}\left[\eta^{-1} I_3(2\beta_1,\eta) - I_3(2\beta_1,1)\right]\right\}.
\end{aligned}
\tag{4.38}
$$

The following notations are introduced in the expressions for the kernels (4.38):

$$
\begin{aligned}
I_1(\beta,\eta) &= \frac{\beta}{2\xi\eta\left[\zeta^2(\eta)-1\right]},\\
I_2(\beta,\eta) &= I_1(\beta,\eta)\left[4\zeta(\eta) I_1(\beta,\eta) - \frac{1}{\beta}\right],\\
I_3(\beta,\eta) &= 4 I_1^2(\beta,\eta)\left\{2\left[3\zeta^2(\eta)+1\right]\, I_1(\beta,\eta) - \frac{3\zeta(\eta)}{\beta}\right\},\\
I_4(\beta,\eta) &= 12 I_1^2(\beta,\eta)\left\{16\zeta(\eta)\left[\zeta^2(\eta)+1\right]\, I_1^2(\beta,\eta)\right.\\
&\quad \left. - \frac{4}{\beta}\left[3\zeta^2(\eta)+1\right] I_1(\beta,\eta) + \frac{\zeta(\eta)}{\beta^2}\right\},\\
\zeta(\eta) &= \frac{\beta^2+\xi^2+\eta^2}{2\xi\eta}.
\end{aligned}
\tag{4.39}
$$

For the *axisymmetric problem on mode II crack* in a semi-infinite pre-stressed body, when radial shear stresses of $\tau_r(r)$ intensity act on crack faces, in the case of equal roots we obtain such system of Fredholm integral equations of the second kind:

$$
\begin{aligned}
&f(\xi) + \frac{4}{\pi k}\int_0^1 f(\eta) K_{11}(\xi,\eta)\, d\eta - \frac{4}{\pi k}\int_0^1 g(\eta) K_{12}(\xi,\eta)\, d\eta = 0,\\
&g(\xi) + \frac{4}{\pi k}\int_0^1 f(\eta) K_{21}(\xi,\eta)\, d\eta - \frac{4}{\pi k}\int_0^1 g(\eta) K_{22}(\xi,\eta)\, d\eta\\
&\qquad = -\frac{4\xi}{\pi k}\int_0^{\pi/2} q'(\xi\sin\theta)\, d\theta,\\
&q(\xi) = \frac{\sqrt{n_1}\xi}{C_{44} d_1}\tau_r(a\xi),
\end{aligned}
\tag{4.40}
$$

where the kernels are of the form (4.38).

For the *axisymmetric problem on mode III crack* in a semi-infinite pre-stressed body, when tangent torsional loads of $\tau_\theta(r)$ intensity are applied to the crack faces antisymmetrically in respect of the plane of crack location, we obtain Fredholm integral equation of the second kind:

$$\begin{gathered} f(\xi) - \frac{1}{\pi}\int_0^1 f(\eta)\, K(\xi,\eta)\, d\eta = \frac{4\xi}{\pi}\int_0^{\pi/2} t'(\xi\sin\theta)\, d\theta, \\ t(\xi) = \frac{\sqrt{n_3}\xi}{C_{44}}\tau_\theta(a\xi), \end{gathered} \tag{4.41}$$

where

$$K(\xi,\eta) = 8\beta_3\xi^2\left[\frac{1}{\left(4\beta_3^2+\xi^2+\eta^2\right)^2 - 4\xi^2\eta^2} - \frac{1}{\left(4\beta_3^2+\xi^2+1\right)^2 - 4\xi^2}\right]. \tag{4.42}$$

4.4.2 Body with Two Parallel Circular Cracks

Now, we will show the results for the case of non-equal roots of the characteristic equation ($n_1 \neq n_2$); the procedures for non-equal roots ($n_1 = n_2$) are carried out similarly.

By performing procedures similar to those presented in the previous subsection, for the non-axisymmetric problem on a pre-stressed body containing two parallel coaxial circular mode I cracks, we obtain such system of Fredholm integral equations of the second kind

$$\begin{aligned} &\left(s\frac{k}{k_1}+q\right) f_1(\xi) + \left(s\frac{k}{k_1}-q\right) f_2(\xi) + \frac{4}{\pi}\int_0^1 f_1(\eta)\, K_{11}(\xi,\eta)\, d\eta \\ &\quad + \frac{4}{\pi}\int_0^1 f_2(\eta)\, K_{12}(\xi,\eta)\, d\eta + \frac{4}{\pi}\int_0^1 f_3(\eta)\, K_{13}(\xi,\eta)\, d\eta = 0, \\ &\left(s\frac{k}{k_1}-q\right) f_1(\xi) + \left(s\frac{k}{k_1}+q\right) f_2(\xi) + \frac{4}{\pi}\int_0^1 f_1(\eta)\, K_{21}(\xi,\eta)\, d\eta \\ &\quad + \frac{4}{\pi}\int_0^1 f_2(\eta)\, K_{22}(\xi,\eta)\, d\eta + \frac{4}{\pi}\int_0^1 f_3(\eta)\, K_{23}(\xi,\eta)\, d\eta = 0, \\ &s\frac{k}{k_2} f_3(\xi) + \frac{4}{\pi}\int_0^1 f_1(\eta)\, K_{31}(\xi,\eta)\, d\eta + \frac{4}{\pi}\int_0^1 f_2(\eta)\, K_{32}(\xi,\eta)\, d\eta \\ &\quad + \frac{4}{\pi}\int_0^1 f_3(\eta)\, K_{33}(\xi,\eta)\, d\eta = \frac{8\xi}{\pi}\int_0^{\pi/2} u'(\xi\sin\theta)\, d\theta, \end{aligned} \tag{4.43}$$

where

$$u(\xi) = \frac{k_1 \xi^n}{C_{44} k_2} \sigma^{(n)}(a\xi), \quad s = \frac{n_2^{-1/2} d_1 d_2 l_1}{d_1 l_1 - d_2 l_2},$$
$$q = n_3^{-1/2}, k_1 = l_1 \sqrt{n_2}, \quad k_2 = l_2 \sqrt{n_1}, \quad k = k_1 - k_2 \tag{4.44}$$

The kernels in (4.43) are of the form Bogdanov et al. (2017)

$$K_{12}(\xi, \eta) = 2n\xi^{n-1}\eta^{-n-1}\left[-\frac{sk_2}{k_1}\beta_1 S_n(z_{11}) + s\beta_2 S_n(z_{12}) - q\beta_3 S_n(z_{13})\right]$$
$$+ \sqrt{\pi}\frac{\Gamma(n+1)}{\Gamma(n+\frac{1}{2})}\xi^{2n}\left[-\frac{sk_2}{k_1}R_n(2\beta_1, \eta) + sR_n(2\beta_2, \eta) - qR_n(2\beta_3, \eta)\right], \tag{4.45}$$

etc., where

$$\beta_j = \beta n_j^{-1/2} = \frac{h}{a} n_j^{-1/2} = \frac{h_j}{a}, \quad z_{1j} = \frac{4\beta_j^2 + \xi^2 + \eta^2}{2\xi\eta}, \quad j = 1, 2, 3,$$
$$S_n(z) = \frac{Q_n(z) - zQ_{n-1}(z)}{4\left(z^2 - 1\right)}, \quad R_n(b, \eta) = \frac{b}{4\left(b^2 + \eta^2\right)^{n+1}},$$

$Q_n(z)$ is Legendre function of the second kind, and $\Gamma(n)$ is gamma function. Here the geometric parameter $\beta = ha^{-1}$ is the dimensionless half-distance between the cracks.

The procedure of solving axisymmetric problems will be exemplified by the problem on a body containing two mode I cracks, for which boundary conditions are of the form (4.20). The harmonic potential functions involved in (4.8) will be presented as Hankel integral expansions

$$\varphi_1^{(1)}(r, z_1) = \int_0^\infty A(\lambda) e^{-\lambda z_1} J_0(\lambda r) \frac{d\lambda}{\lambda},$$
$$\varphi_2^{(1)}(r, z_2) = \int_0^\infty B(\lambda) e^{-\lambda z_2} J_0(\lambda r) \frac{d\lambda}{\lambda},$$
$$\varphi_1^{(2)}(r, z_1) = \int_0^\infty [C_1(\lambda)\cosh\lambda\ (z_1 + h_1) + C_2(\lambda)\sinh\lambda\ (z_1 + h_1)] J_0(\lambda r) \frac{\partial\lambda}{\lambda\sinh\mu_1},$$
$$\varphi_2^{(2)}(r, z_2) = \int_0^\infty [D_1(\lambda)\cosh\lambda(z_2 + h_2) + D_2(\lambda)\sinh\lambda(z_2 + h_2)] J_0(\lambda r) \frac{\partial\lambda}{\lambda\sinh\mu_2}, \tag{4.46}$$

where A, B, C_k, and D_k $(k = 1, 2)$ are unknown functions that are to be determined; $\mu_k = \lambda h_k = \lambda h n_k^{-1/2}$.

Substitute expressions (4.46) into boundary conditions (4.20). Then, from the conditions presented in the second and fourth lines of (4.20), which are set on all planes $y_3 = -h$, $y_3 = 0$, we obtain four relations linking six functions A, B, C_k, and D_k $(k = 1, 2)$

$$
\begin{aligned}
A(\lambda) &= \frac{1}{k}\left[(k_2 + k_1 \coth\mu_1)\, C_1(\lambda) + \frac{d_2 l_2}{d_1 l_1} k_1 (1 + \coth\mu_2)\, D_1(\lambda)\right], \\
B(\lambda) &= -\frac{1}{k}\left[\frac{d_1 l_1}{d_2 l_2} k_2 (1 + \coth\mu_1)\, C_1(\lambda) + (k_1 + k_2 \coth\mu_2)\, D_1(\lambda)\right], \\
C_2(\lambda) &= 0, \quad D_2(\lambda) = 0.
\end{aligned}
\tag{4.47}
$$

From the remaining boundary conditions (4.20), the following system of paired (dual) integral equations is obtained

$$
\begin{aligned}
\int_0^\infty [d_1 l_1 \coth\mu_1\, C_1(\lambda) + d_2 l_2 \coth\mu_2\, D_1(\lambda)]\, J_0(\lambda r)\, \lambda d\lambda &= -\frac{\sigma(r)}{C_{44}}, \quad r \leqslant a, \\
\int_0^\infty \left[n_1^{-1/2} d_1 C_1(\lambda) + n_2^{-1/2} d_2 D_1(\lambda)\right] J_1(\lambda r)\, \lambda d\lambda &= 0, \quad r \leqslant a, \\
\int_0^\infty X_1 J_0(\lambda r)\, d\lambda &= 0, \quad r > a, \\
\int_0^\infty X_2 J_1(\lambda r)\, d\lambda &= 0, \quad r > a,
\end{aligned}
\tag{4.48}
$$

where

$$
\begin{aligned}
X_1 &= \frac{d_1 l_1}{d_2 l_2}(1 + \coth\mu_1)\, C_1(\lambda) + (1 + \coth\mu_2)\, D_1(\lambda), \\
X_2 &= \frac{d_1}{d_2}\sqrt{\frac{n_2}{n_1}}(1 + \coth\mu_1)\, C_1(\lambda) + (1 + \coth\mu_2)\, D_1(\lambda).
\end{aligned}
$$

Functions X_1 and X_2 are presented in the form permitting two last equations in (4.48) (for the range $r > a$) to be satisfied identically, viz.,

$$
\begin{aligned}
X_1 &= \sqrt{\frac{\pi\lambda}{2}} \int_0^a \sqrt{t}\varphi(t)\, J_{1/2}(\lambda t)\, dt \\
&= \int_0^a \varphi(t) \sin\lambda t\, dt, \\
X_2 &= \sqrt{\frac{\pi\lambda}{2}} \int_0^a \sqrt{t}\psi(t)\, J_{3/2}(\lambda t)\, dt,
\end{aligned}
\tag{4.49}
$$

where $\varphi(t)$ and $\psi(t)$ are unknown functions continuous along with their first derivatives in the segment $[0, a]$. In that case, from the first two equations in (4.48) we obtain the system of Fredholm integral equations of the second kind

$$
\begin{aligned}
f(\xi) + \frac{2}{\pi k}\int_0^1 f(\eta)\, K_{11}(\xi, \eta)\, d\eta + \frac{2}{\pi k}\int_0^1 g(\eta)\, K_{12}(\xi, \eta)\, d\eta \\
= -\frac{4}{\pi}\int_0^{\pi/2} s(\xi \sin\theta)\, d\theta, \\
g(\xi) + \frac{2}{\pi k}\int_0^1 f(\eta)\, K_{21}(\xi, \eta)\, d\eta + \frac{2}{pk}\int_0^1 g(\eta)\, K_{22}(\xi, \eta)\, d\eta = 0,
\end{aligned}
\tag{4.50}
$$

where

$$f(\xi) \equiv a^{-1}\varphi(a\xi), \quad g(\xi) \equiv a^{-1}\frac{d}{d\xi}[\xi\psi(a\xi)], \\ s(\xi) = \frac{\xi}{C_{44}d_2l_2}\sigma(a\xi). \tag{4.51}$$

The kernels are of the form:

$$\begin{aligned} K_{11}(\xi,\eta) &= k_1 I_1(2\beta_1,\eta) - k_2 I_1(2\beta_2,\eta), \\ K_{12}(\xi,\eta) &= k_1\{[I_0(2\beta_1,1) - I_0(2\beta_2,1)] \\ &\quad - \eta^{-1}[I_0(2\beta_1,\eta) - I_0(2\beta_2,\eta)]\}, \\ K_{21}(\xi,\eta) &= -k_2\xi[I_2(2\beta_1,\eta) - I_2(2\beta_2,\eta)], \\ K_{22}(\xi,\eta) &= -\xi\{[k_2 I_1(2\beta_1,1) - k_1 I_1(2\beta_2,1)] \\ &\quad - \eta^{-1}[k_2 I_1(2\beta_1,\eta) - k_1 I_1(2\beta_2,\eta)]\}, \end{aligned} \tag{4.52}$$

where

$$I_0(\beta,\eta) = \frac{1}{4}\ln\frac{\zeta(\eta)+1}{\zeta(\eta)-1},$$

$I_1(\beta,\eta)$, $I_2(\beta,\eta)$, and $\zeta(\eta)$ are determined from (4.39), and k_1, k_2, and k—from (4.44).

By performing similar procedures for the axisymmetric problem on mode II cracks in an unbounded body the following system of Fredholm integral equations of the second kind is obtained

$$\begin{aligned} f(\xi) - \frac{2}{\pi k}\int_0^1 f(\eta)K_{11}(\xi,\eta)\,d\eta - \frac{2}{\pi k}\int_0^1 g(\eta)K_{12}(\xi,\eta)\,d\eta &= 0, \\ g(\xi) - \frac{2}{\pi k}\int_0^1 f(\eta)K_{21}(\xi,\eta)\,d\eta - \frac{2}{\pi k}\int_0^1 g(\eta)K_{22}(\xi,\eta)\,d\eta &= \\ = \frac{4}{\pi}\xi\int_0^{\pi/2} q'(\xi\sin\theta)\,d\theta, \end{aligned} \tag{4.53}$$

where

$$q(\xi) = \frac{\sqrt{n_2}\xi}{C_{44}d_2}\tau_r(a\xi), \tag{4.54}$$

and the kernels are determined from (4.52).

For the axisymmetric problem on mode III cracks in an unbounded body, such Fredholm integral equation of the second kind is obtained

$$f(\xi) + \frac{1}{\pi}\int_0^1 f(\eta)K(\xi,\eta)\,d\eta = \frac{4\xi}{\pi}\int_0^{\pi/2} t'(\xi\sin\theta)\,d\theta, \\ t(\xi) = \frac{\sqrt{n_3}\xi}{C_{44}}\tau_\theta(a\xi), \tag{4.55}$$

where the kernel is of the form (4.42).

4.5 Stress Intensity Factors

Now we analyze the asymptotic distribution of stresses in the vicinities of crack edges in the investigated pre-stressed bodies containing cracks and determine stress intensity factors (*SIFs*), which like those in classical fracture mechanics (Cherepanov 1979; Kassir and Sih 1975) are coefficients at singularities in the stress distributions mentioned when approaching crack edges.

4.5.1 Half-Space with a Near-Surface Circular Crack

The procedure of determining stress intensity factors for the non-axisymmetric problem on a body with a near-surface circular crack will be considered in more detail.

From the representations of stresses via harmonic potential functions (4.9), given (4.27), (4.28), and (4.30), we obtain expressions for stress tensor components Q'_{33}, Q'_{3r}, and $Q'_{3\theta}$ in the domain $y_3 = 0, r > a$ (i.e., in the plane of crack location, outside its contour, in subdomain "2"). For Q'_{33} we have

$$Q'^{(2)}_{33}(r,\theta,0) = \tfrac{1}{4}C_{44}skl_1\sqrt{n_1}\sum_{n=0}^{\infty}\cos n\theta\ \left\{\int_0^{\infty} X_3 J_n(\lambda r)\lambda d\lambda\right.$$
$$\left. - \frac{2}{k^2}\int_0^{\infty}\left[\mu_1^2(X_1+X_2)+\left(\frac{k^2}{2}+\mu_1^2+\mu_1 k\right)X_3\right]e^{-2\mu_1}J_n(\lambda r)\lambda d\lambda\right\}. \tag{4.56}$$

The analysis of expression (4.56) implies that the singularity when $r \to a$ only involves the first integral in the braces since in the second integral in the braces, as follows from the corresponding formulas of Bessel function integrals (Prudnikov et al. 1986b), this singularity is absent. In this connection, the first integral in braces in (4.56) will be analyzed in more detail. Given expressions (4.31) and formulas (4.33), performing integration by parts and taking into account the value of discontinuous integral (4.32), we obtain

$$\int_0^{\infty} X_3 J_n(\lambda r)\lambda d\lambda$$
$$= \sqrt{\frac{\pi}{2}}\int_0^{\infty}\left[\int_0^a \sqrt{t}\omega(t)\,\lambda J_{n+1/2}(\lambda t)\,dt\right]J_n(\lambda r)\sqrt{\lambda}d\lambda$$
$$= -\frac{a^n\omega(a)}{r^n\sqrt{r^2-a^2}} + \int_0^a \frac{\tilde{\omega}(t)\,dt}{r^n\sqrt{r^2-t^2}}. \tag{4.57}$$

The integral

$$\int_0^a \frac{\tilde{\omega}(t)\,dt}{r^n\sqrt{r^2-t^2}}$$

does not have singularities when $r \to a$ (Prudnikov et al. 1986a). Then from (4.56) and (4.57), taking into account the expression

$$\omega(t) = t^{-n}\int_0^t \tilde{\omega}(t)\,dt,$$

we obtain

$$Q_{33}^{\prime(2)}(r,\theta,0) = -\tfrac{1}{4}C_{44}skl_1\sqrt{n_1}\sum_{n=0}^{\infty}\cos n\theta \times \left[\int_0^a \tilde{\omega}(t)\,dt\right]\frac{r^{-n}}{\sqrt{(r-a)(r+a)}} + O(1), \quad (4.58)$$

where symbol $O(1)$ denotes regular components that do not have singularities when $r \to a$.

Performing a similar analysis for other stress tensor components in the plane of crack location, we obtain

$$Q_{3r}^{\prime(2)}(r,\theta,0) = \tfrac{1}{4}C_{44}sk\sum_{n=0}^{\infty}\cos n\theta\,\frac{r^{-n+1}}{\sqrt{(r-a)(r+a)}} \times \left[\frac{\tilde{\varphi}(a)}{a} + a^{n-1}\psi(a)\right] + O(1), \quad (4.59)$$

$$Q_{3\theta}^{\prime(2)}(r,\theta,0) = \tfrac{1}{4}C_{44}q\sum_{n=1}^{\infty}\sin n\theta\,\frac{r^{-n+1}}{\sqrt{(r-a)(r+a)}} \times \left[\frac{\tilde{\varphi}(a)}{a} - a^{n-1}\psi(a)\right] + O(1). \quad (4.60)$$

Expressions (4.58)–(4.60) can be written as

$$\begin{aligned} Q_{33}^{\prime(2)}(r,\theta,0) &= \frac{K_I}{\sqrt{2\pi(r-a)}} + O(1),\\ Q_{3r}^{\prime(2)}(r,\theta,0) &= \frac{K_{II}}{\sqrt{2\pi(r-a)}} + O(1),\\ Q_{3\theta}^{\prime(2)}(r,\theta,0) &= \frac{K_{III}}{\sqrt{2\pi(r-a)}} + O(1). \end{aligned} \quad (4.61)$$

In (4.61), stress intensity factors (*SIFs*) are expressed by the following relations

$$
\begin{aligned}
K_I &= -\tfrac{1}{4}C_{44}skl_1\sqrt{n_1}\sqrt{\frac{\pi}{a}}\sum_{n=0}^{\infty}\cos n\theta\ \left[a^{-n}\int_0^a \tilde{\omega}\,(t)\,dt\right] \\
&= -\tfrac{1}{4}C_{44}skl_1\sqrt{n_1}\sqrt{\pi a}\sum_{n=0}^{\infty}\cos n\theta\ \int_0^1 f_3\,(\eta)\,d\eta, \\
K_{II} &= \tfrac{1}{4}C_{44}sk\sqrt{\frac{\pi}{a}}\sum_{n=0}^{\infty}\cos n\theta\ \left\{a^{-n+1}\left[\frac{\tilde{\omega}\,(a)}{a}+a^{n-1}\psi\,(a)\right]\right\} \\
&= \tfrac{1}{4}C_{44}sk\sqrt{\pi a}\sum_{n=0}^{\infty}\cos n\theta\ \left[f_1\,(1)+f_2\,(1)\right], \\
K_{III} &= \tfrac{1}{4}C_{44}q\sqrt{\pi a}\sum_{n=1}^{\infty}\sin n\theta\ \left\{a^{-n+1}\left[\frac{\tilde{\omega}\,(a)}{a}-a^{n-1}\psi\,(a)\right]\right\} \\
&= \tfrac{1}{4}C_{44}q\sqrt{\pi a}\sum_{n=1}^{\infty}\sin n\theta\ \left[f_1\,(1)-f_2\,(1)\right],
\end{aligned}
\tag{4.62}
$$

where functions $f_1\,(\xi)$, $f_2\,(\xi)$, and $f_3\,(\xi)$ are determined by solving the system of Fredholm integral equations (4.34).

Expressions (4.61) and (4.62) imply that the order of singularity in stresses distribution in the vicinity of a near-surface crack edge in a semi-infinite pre-stressed body is $-1/2$, i.e., it coincides with the order of singularity in stresses distribution near the crack edge in a body free of initial stresses (Kassir and Sih 1975). In addition, it follows from (4.62) that the mutual influence of a near-surface crack and material's free surface causes qualitative changes in the asymptotic distribution of stresses near the crack edge, viz., non-zero values of K_{II} and K_{III} in the case of loading crack faces only by normal forces (when $\sigma\,(r,\theta)\neq 0$, $\tau_r(r,\theta)=\tau_\theta(r,\theta)=0$) (in the problem on a body containing an isolated mode I crack $K_I\neq 0$, $K_{II}=0$, and $K_{III}=0$ (Bogdanov et al. 2017)) and non-zero values of K_I in the case when only tangent shear forces $\tau_r(r,\theta)$ act on crack faces (for such scheme of loading the faces of an isolated crack in an unbounded body, it was $K_I=0$, $K_{II}\neq 0$, and $K_{III}=0$ (Bogdanov et al. 2017)). Besides, it can be seen from expressions (4.62) that all three *SIFs* depend on initial stresses, since parameters C_{44}, s, k, q, l_1, and n_1 depend on the elongation (contraction) coefficient λ_1, which, in turn, is determined by the action of initial stresses $S_{11}^0=S_{22}^0$.

Analyze the limit case of mode I crack location, when the distance between the crack and half-space boundary tends to infinity. It follows from the analysis of expressions (4.36) for the kernels of integral equations (4.34) that when $\beta\to\infty$, all the kernels in the limit become zero. Then (4.34) implies

$$
\begin{aligned}
&f_1^{\infty}=f_2^{\infty}=0, \\
&f_3^{\infty}=-\frac{8}{\pi sk}\xi\int_0^{\pi/2}u'\,(\xi\sin\theta\,)\,d\theta, \\
&f_j^{\infty}\equiv\lim_{\beta\to\infty}f_j\,,\quad j=1,2,3.
\end{aligned}
\tag{4.63}
$$

From (4.63), taking into account (4.35) and performing the change of variables $\eta = \xi \sin\theta$, we obtain

$$f_3^{\infty} = -\frac{8}{\pi C_{44} s k l_1 \sqrt{n_1}} \frac{d}{d\xi} \int_0^{\xi} \frac{\eta^{n+1} \sigma^{(n)}(a\eta)}{\sqrt{\xi^2 - \eta^2}} d\eta.$$

Then, we have from (4.62)

$$\begin{aligned} K_I^{\infty} &\equiv \lim_{\beta \to \infty} K_I \\ &= 2\sqrt{\frac{a}{\pi}} \sum_{n=0}^{\infty} \cos n\theta \int_0^1 \frac{\eta^{n+1} \sigma^{(n)}(a\eta)}{\sqrt{1-\eta^2}} d\eta \\ &= \frac{2}{\sqrt{\pi a}} \sum_{n=0}^{\infty} \frac{\cos n\theta}{a^n} \int_0^a \frac{t^{n+1} \sigma^{(n)}(t)}{\sqrt{a^2 - t^2}} dt, \\ K_{II}^{\infty} &= 0, \\ K_{III}^{\infty} &= 0, \end{aligned} \tag{4.64}$$

where Fourier coefficients $\sigma^{(n)}(x)$ $(n = 0, 1, 2, \dots)$ are determined from relations (4.26) via the normal load acting on the crack faces.

As can be seen, in this case *SIFs* do not depend on initial stresses and entirely coincide with the values obtained in the non-axisymmetric problem on a mode I crack in an infinite pre-stressed body (Bogdanov et al. 2017). In particular, when normal loads of the form

$$\sigma(r, \theta) = \sigma_1 \cos\theta \tag{4.65}$$

are applied to crack faces, we obtain

$$K_I^{\infty} = \tfrac{1}{2}\sqrt{\pi a}\sigma_1 \cos\theta\,, \quad K_{II}^{\infty} = 0, \quad K_{III}^{\infty} = 0. \tag{4.66}$$

It should be noted that the values of *SIFs* obtained by solving the problem on a pre-stressed body containing a near-surface mode I crack in the limit case of crack location, when the distance between it and the half-space boundary tends to infinity (those *SIF* values are given by expressions (4.64) and (4.66)) also entirely coincide with the values of *SIFs* which were obtained in the non-axisymmetric problem on an infinite body with a penny-shaped mode I crack within fracture mechanics of materials free of initial stresses (Kassir and Sih 1975).

By performing similar procedures in the case of axisymmetric problem on a half-space containing a near-surface mode I crack (Bogdanov et al. 2017), we obtain such expressions for stress tensor components near the crack edge:

$$\begin{aligned} Q_{33}^{\prime(2)}(r,0) &= \frac{K_I}{\sqrt{2\pi(r-a)}} + O(1), \\ Q_{3r}^{\prime(2)}(r,0) &= \frac{K_{II}}{\sqrt{2\pi(r-a)}} + O(1), \\ Q_{3\theta}^{\prime(2)}(r,0) &= 0. \end{aligned} \tag{4.67}$$

In (4.67), *SIFs* are determined from the expressions

$$\begin{aligned} K_I &= -\tfrac{1}{2} C_{44} k d_1 l_1 \sqrt{\pi a}\, f(1), \\ K_{II} &= -\tfrac{1}{2} C_{44} k d_1 n_1^{-1/2} \sqrt{\pi a} \int_0^1 g(\eta)\, d\eta, \\ K_{III} &= 0, \end{aligned} \tag{4.68}$$

where functions f and g are determined by solving the system of Fredholm integral equations (4.37). It can also be shown that in the limit case of crack location, when the distance between the crack and the half-space boundary tends to infinity, we have

$$\begin{aligned} K_I^{\infty} &= 2\sqrt{\frac{a}{\pi}} \int_0^1 \frac{\eta s(\eta)}{\sqrt{1-\eta^2}} d\eta = \frac{2}{\sqrt{\pi a}} \int_0^a \frac{t\sigma(t)}{\sqrt{a^2-t^2}} dt, \\ K_{II}^{\infty} &= 0, \\ K_{III}^{\infty} &= 0. \end{aligned} \tag{4.69}$$

In particular, when uniform normal pressure of the form

$$\sigma(r) = \sigma = \text{const}, \tag{4.70}$$

acts on crack faces, we have from (4.69)

$$K_I^{\infty} = 2\sigma\sqrt{\frac{a}{\pi}}. \tag{4.71}$$

In the case of the axisymmetric problem on a half-space containing a near-surface mode II crack, *SIFs* are of the form (4.68), where functions f and g are determined by solving the system of Fredholm integral equations (4.40). In the limit case of crack location, when the distance between the crack and the half-space boundary tends to infinity, we have

$$\begin{aligned} K_I^{\infty} &= 0, \\ K_{II}^{\infty} &= 2\sqrt{\frac{a}{\pi}} \int_0^1 \frac{\eta^2 q(\eta)}{\sqrt{1-\eta^2}} d\eta = \frac{2}{a\sqrt{\pi a}} \int_0^a \frac{t^2 \tau_r(t)}{\sqrt{a^2-t^2}} dt, \\ K_{III}^{\infty} &= 0. \end{aligned} \tag{4.72}$$

In particular, when a uniform shear load of the form

$$\tau_r\,(r) = \tau = \text{const}, \tag{4.73}$$

acts on the crack faces, we have from (4.72)

$$K_{II}^{\infty} = \frac{\tau}{2}\sqrt{\pi a}. \tag{4.74}$$

In the case of the axisymmetric problem on a half-space containing a near-surface mode III crack, *SIFs* are of the form Bogdanov et al. (2017):

$$K_I = 0, \quad K_{II} = 0, \quad K_{III} = \tfrac{1}{2}C_{44}n_3^{-1/2}\sqrt{\pi a}\int_0^1 f\,(\eta)\,d\eta, \tag{4.75}$$

where function f is determined by solving Fredholm integral equation (4.41). In the limit case of crack location, when the distance between the crack and the half-space boundary tends to infinity, we have

$$\begin{aligned} K_I^{\infty} &= 0, \\ K_{II}^{\infty} &= 0, \\ K_{III}^{\infty} &= 2\sqrt{\frac{a}{\pi}}\int_0^1 \frac{\eta^2 t(\eta)}{\sqrt{1-\eta^2}}d\eta = \frac{2}{a\sqrt{\pi a}}\int_0^a \frac{t^2\tau_\theta(t)}{\sqrt{a^2-t^2}}dt. \end{aligned} \tag{4.76}$$

In particular, when a uniform torsional load of the form

$$\tau_\theta\,(r) = \tau = \text{const} \tag{4.77}$$

acts on the crack faces, we have from (4.76)

$$K_{III}^{\infty} = \frac{\tau}{2}\sqrt{\pi a}. \tag{4.78}$$

It should be noted that from the analysis of the asymptotic distribution of stresses in the vicinity of the near-surface crack edge we can make conclusions concerning the order of singularities near the crack edges, the influence of initial stresses on stress intensity factors, as well as the effect of crack interaction with the body boundary, which are similar to those made in the consideration of the non-axisymmetric problem.

4.5.2 *Body with Two Parallel Circular Cracks*

For the non-axisymmetric problem on a pre-stressed body containing two parallel coaxial mode I cracks, in the case of non-equal roots ($n_1 \neq n_2$) we obtain the asymptotic distribution of stress tensor components as (4.61) with *SIFs* of the forms

$$
\begin{aligned}
K_I &= C_{44}\frac{sk}{4k_1}\sqrt{\pi a}\sum_{n=0}^{\infty}\cos n\theta \int_0^1 f_3(\eta)\,d\eta,\\
K_{II} &= C_{44}\frac{sk}{4k_1}\sqrt{\pi a}\sum_{n=0}^{\infty}\cos n\theta\ [f_1(1)+f_2(1)],\\
K_{III} &= \tfrac{1}{4}C_{44}q\sqrt{\pi a}\sum_{n=1}^{\infty}\sin n\theta\ [f_1(1)-f_2(1)],
\end{aligned}
\tag{4.79}
$$

where functions $f_1(\xi)$, $f_2(\xi)$, and $f_3(\xi)$ are determined by solving the system of Fredholm integral equations (4.43). It is seen from (4.79) that the effect of mutual influence of two parallel coaxial cracks in a pre-stressed body is evident in the appearance of non-zero values of ${K_{II}}^{\infty}$ and ${K_{III}}^{\infty}$ only under the action of a normal load on crack faces. It can also be shown that when the distance between cracks tends to infinity, in the limit we obtain the values of *SIFs* ${K_I}^{\infty}$, ${K_{II}}^{\infty}$, and ${K_{III}}^{\infty}$ as (4.64) (while for the special case of a non-axisymmetric normal load acting on crack faces (4.65) the values of *SIFs* are of the form (4.66)), which corresponds to physical considerations.

For the axisymmetric problem on two parallel coaxial mode I cracks located in a pre-stressed body, we obtain expressions for stress tensor components in the vicinities of cracks as (4.67), where *SIFs* are presented by the expressions

$$
\begin{aligned}
K_I &= -\tfrac{1}{2}C_{44}d_2l_2f(1),\\
K_{II} &= \tfrac{1}{2}C_{44}d_2n_2^{-1/2}\int_0^1 g(\eta)\,d\eta,\\
K_{III} &= 0,
\end{aligned}
\tag{4.80}
$$

while functions f and g are determined by solving the system of Fredholm integral equations (4.50). In the limit case of cracks location, when the distance between them tends to infinity, we arrive at the values of *SIFs* of the form (4.69) (and in the special case of the load acting on cracks faces as (4.70), ${K_I}^{\infty}$ is of the form (4.71)).

By solving the axisymmetric problem on two parallel coaxial mode II cracks located in a pre-stressed body we obtain expressions for *SIFs* in the form of (4.79), where functions f and g are determined from the solution of the system of Fredholm integral equations (4.53). In the limit case of cracks location, when the distance between them tends to zero, we arrive at the values of *SIFs* as (4.72) (while in the special case of the load on cracks faces (4.73), ${K_{II}}^{\infty}$ is of the form of (4.74)).

Finally, when considering the axisymmetric problem on a pre-stressed body containing two parallel mode III cracks, we arrive at the values of *SIFs* as (4.75), where functions f and g are determined from the solution of Fredholm integral equation (4.55). In the limit case of cracks location, when the distance between them tends to infinity, we obtain the values of *SIFs* as (4.76) (while in the special case of the torsional load of the form (4.77) acting on cracks faces, the value of ${K_{III}}^{\infty}$ is of the form (4.78)).

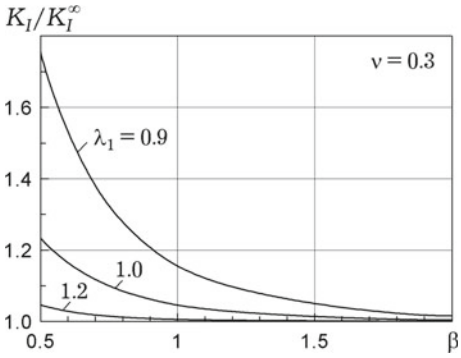

Fig. 4.4 Dependence of *SIFs* ratios K_I/K_I^∞ on the dimensionless distance between the crack and the boundary surface of the body $\beta = ha^{-1}$ for the harmonic-type potential

4.6 Numerical Results

Below we present the results of numerical investigation for some highly elastic materials and composites. The parameters of those materials, which are involved in the resolving Fredholm integral equations of the second kind, and expressions for stress intensity factors are given, e.g., in Bogdanov et al. (2017), Guz et al. (2020).

Highly elastic material with the elastic potential of harmonic type (a compressible body, equal roots) (John 1960). Consider the results of numerical calculation for the non-axisymmetric problem on a body containing a near-surface mode I crack, when crack faces are under a normal tensile load of (4.65) form.

Figure 4.4 shows the dependence of the stress intensity factors (*SIFs*) ratios K_I/K_I^∞ on the dimensionless distance between the crack and the half-space boundary $\beta = ha^{-1}$ for the value of Poisson coefficient $\nu = 0.3$. Here, K_I^∞ is determined from (4.66) and corresponds to the *SIF* value in the problem on an isolated mode I crack in an infinite pre-stressed body (this value, as shown in Sect. 4.5.1, coincides with the *SIF* value in the problem on a mode I crack in a body free of initial stresses). The dependences are given for the values of $\lambda_1 = 0.9$ (initial compression), $\lambda_1 = 1.2$ (initial tension) and $\lambda_1 = 1.0$ (no initial stresses). It can be seen that the interaction of the crack and the free body boundary increases substantially when the distance between them decreases. E.g., for $\lambda_1 = 0.9$ the value of $K_I/K_I{}^\infty$ when $\beta = 0.5$ is higher than the corresponding value of $K_I/K_I{}^\infty$ when $\beta = 2.0$ by a factor of 1.7. On the other hand, with the increase in the distance between the crack and the half-space boundary this mutual influence weakens rapidly, and the respective values of *SIFs* tend to the values obtained for an isolated crack in an infinite body. The precision acceptable for practical calculations, the mutual influence between the crack and the free surface can be neglected when the distance between them exceeds 2 crack radii.

Figure 4.5 illustrates the dependence of $K_I/K_I{}^\infty$ on the parameter of initial stresses λ_1 for different values of Poisson coefficient ν when $\beta = 0.5$. As can be seen from the figure, the compressibility of the material with harmonic-type potential, which is characterized by Poisson coefficient, noticeably influences the values of *SIFs*. E.g., when $\lambda_1 = 0.95$, $\beta = 0.5$, the value of $K_I/K_I{}^\infty$ for $\nu = 0.5$ exceeds

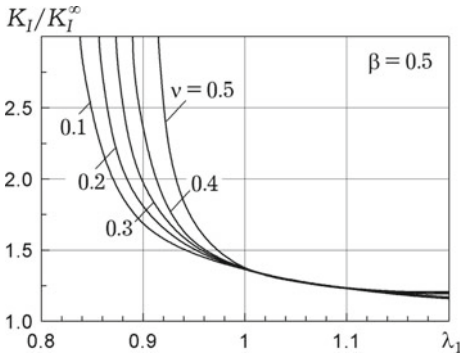

Fig. 4.5 Dependence of *SIFs* ratios K_I/K_I^∞ on elongation (or contraction) ratio λ_1 for different values of Poisson's ratio (the harmonic-type elastic potential)

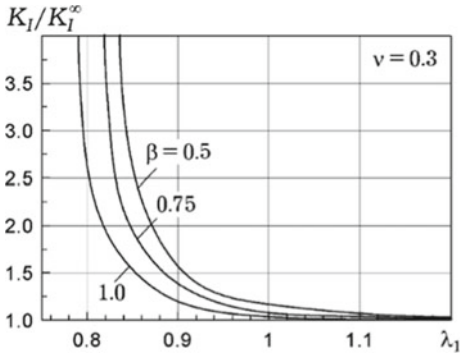

Fig. 4.6 Dependence of *SIFs* ratios K_I/K_I^∞ on elongation (or contraction) ratio λ_1 for the harmonic-type potential

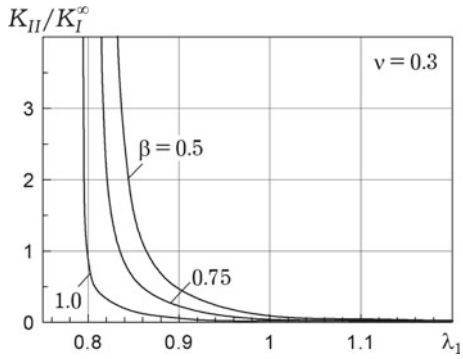

Fig. 4.7 Dependence of *SIFs* ratios K_{II}/K_I^∞ on elongation (or contraction) ratio λ_1 for the harmonic-type potential

the value of $K_I/K_I{}^\infty$ for $\nu = 0.1$ by 12%, while for $\lambda_1 = 0.9$, $\beta = 0.5$ these values differ by a factor of 2.2.

Figures 4.6, 4.7, and 4.8 show, respectively, the dependences of $K_I/K_I{}^\infty$, $K_{II}/K_I{}^\infty$, and $K_{III}/K_I{}^\infty$ on the parameter of initial elongation (contraction) λ_1 at different values of geometric parameter $\beta = ha^{-1}$ for the value of Poisson coefficient $\nu = 0.3$. As the figures imply, *SIFs* considerably depend on initial stresses, with the influence of contractive initial stresses being higher than that of tensile stresses.

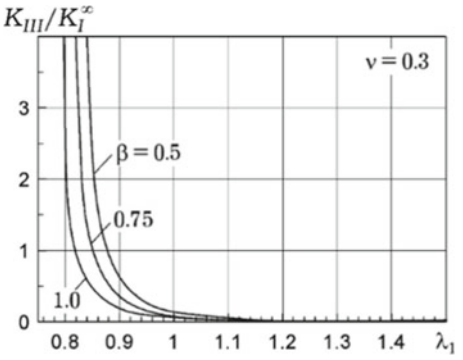

Fig. 4.8 Dependence of *SIFs* ratios K_{III}/K_I^{∞} on elongation (or contraction) ratio λ_1 for the harmonic-type potential

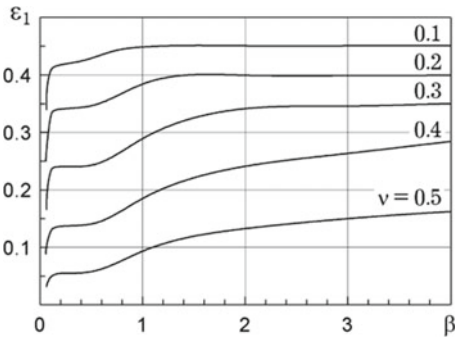

Fig. 4.9 Dependence of the critical values of relative contraction ε_1 on the geometric parameter β for the harmonic-type potential (non-axisymmetric form of stability loss)

The curves in Figs. 4.6, 4.7, and 4.8 have vertical asymptotes corresponding to a sharp (resonance) increase of the stress intensity factors at certain values of the initial contraction parameter $\lambda_1 < 1$. According to the unified approach within the linearized mechanics of deformable solid bodies, described in Sect. 4.1, this effect permits determining the critical (limit) values of contraction parameters, which, when achieved, cause local loss of material's stability in the vicinity of the crack.

Figure 4.9 shows for different values of Poisson coefficient the dependences of the values of relative critical contraction $\varepsilon_1 = 1 - \lambda_1$ corresponding to the local loss of material's stability in the vicinity of near-surface crack in the non-axisymmetric form (the first harmonic in coordinate θ) of the geometric parameter $\beta = ha^{-1}$. The figure implies that the mutual influence of the crack and the half-space boundary leads to a substantial decrease in the values of ε_1 and, respectively, in the critical contraction stresses as compared to the case of a single isolated crack in an unbounded body (in this case for the harmonic-type potential, critical contractions corresponding to the non-axisymmetric form of stability loss are calculated by the formula $\varepsilon_1 = (1 - \nu)/2$ (Guz et al. 1992, 2020)). At the same time, with an increase in the distance between the crack and the half-space boundary this influence becomes weaker, and corresponding critical parameters tend to the values obtained for the case of a single crack in a body.

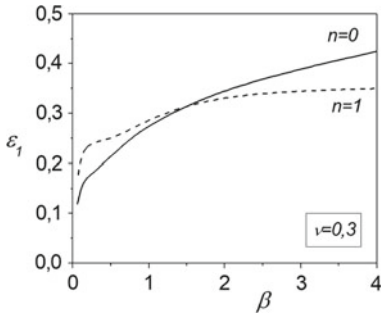

Fig. 4.10 Comparing the critical values ε_1 in the cases of the axisymmetric and non-axisymmetric forms of stability loss for the harmonic-type potential

Figure 4.10 compares for the same material the dependences of ε_1 on β that were obtained from the solution of the axisymmetric problem (the axisymmetric form of stability loss, solid line) and from the solution of the non-axisymmetric problem (the non-axisymmetric form of stability loss, dashed line). It should be noted here that the critical contractions corresponding to the axisymmetric form of stability loss are calculated for the harmonic-type potential with the formula $\varepsilon_1 = 1/(2+\nu)$ (Guz et al. 1992, 2020).

Highly elastic material with Bartenev–Khazanovich elastic potential (an incompressible body, equal roots) (Bartenev and Khazanovich 1960). The results of investigating the axisymmetric problems on a pre-stressed body containing two parallel coaxial cracks for this material are given here.

Figures 4.11 and 4.12 illustrate for mode I cracks, when forces of the form (4.70) act on crack faces, the dependences of the ratios of stress intensity factors K_I/K_I^{∞} and K_{II}/K_I^{∞}, respectively, (here K_I^{∞} is determined from (4.71)) on the parameter of initial stresses λ_1 for different values of the dimensionless half-distance between the cracks $\beta = ha^{-1}$. It can be seen from the figures that *SIFs* K_I, K_{II} significantly depend on initial stresses. The curves shown in Figs. 4.11 and 4.12 have vertical asymptotes that correspond to the effect of resonance nature, when the initial contraction stresses (and, correspondingly, the parameter of initial contraction $\lambda_1 < 1$) achieve the values at which the local loss of material's stability occurs (in the form symmetric with respect to the plane $y_3 = -h$) in the vicinity of cracks under contraction along the cracks.

Figures 4.13 and 4.14 for mode II cracks, when forces of (4.73) form act on crack faces, show, respectively, the dependences of the ratios of the *SIFs* K_{II}/K_{II}^{∞} and K_I/K_{II}^{∞} (where K_{II}^{∞} is determined from (4.74)) on the parameter of initial stresses λ_1 for different values of the dimensionless half-distance between the cracks) $\beta = ha^{-1}$. The figures demonstrate the significant influence of initial stresses on *SIFs* K_I and K_{II}.

In the domain of compressive initial stresses ($\lambda_1 < 1$), the curves have vertical asymptotes corresponding to the resonance *SIF* change occurring when the values of initial compressive stresses tend to the values at which the local loss of material's stability in the vicinity of cracks occurs (in the antisymmetric in respect of plane $y_3 = -h$, or bending, form) under compression by forces directed along the cracks.

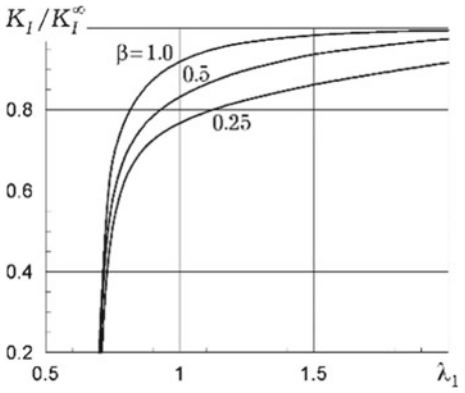

Fig. 4.11 Dependence of *SIFs* ratios $K_I/K_I{}^{\infty}$ on elongation (or contraction) ratio λ_1 for Bartenev–Khazanovich potential

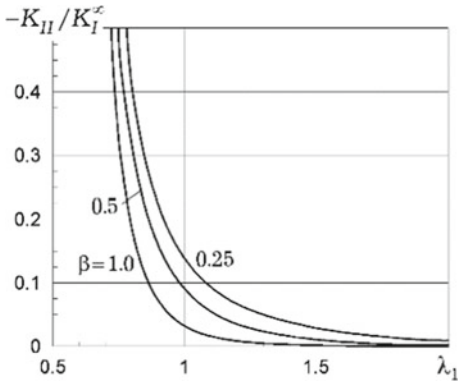

Fig. 4.12 Dependence of *SIFs* ratios $K_{II}/K_I{}^{\infty}$ on elongation (or contraction) ratio λ_1 for Bartenev–Khazanovich potential

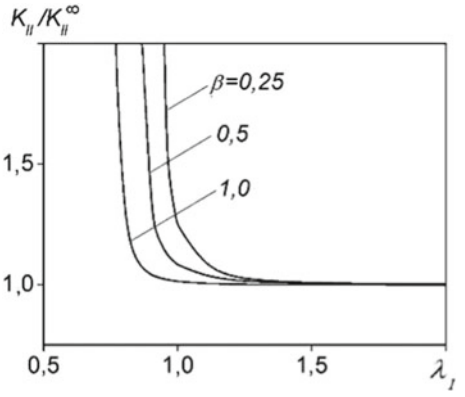

Fig. 4.13 Dependence of *SIFs* ratios K_{II}/K_{II}^{∞} on elongation (or contraction) ratio λ_1 for Bartenev–Khazanovich potential

Here, it should be noted that the critical (limit) values of contraction parameters $\lambda_1 < 1$ for the antisymmetric (bending) form of stability loss are larger (and the critical (limit) compressive stresses, correspondingly, smaller) than the critical values for the symmetric form of stability loss which were obtained above (see Figs. 4.11

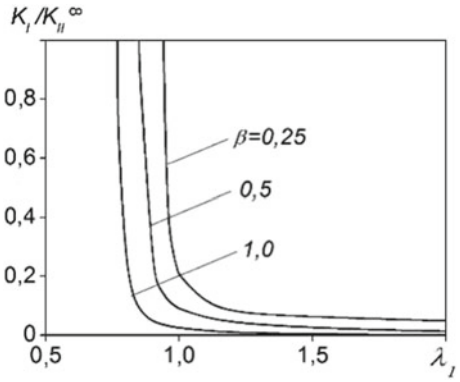

Fig. 4.14 Dependence of *SIFs* ratios K_I/K_{II}^{∞} on elongation (or contraction) ratio λ_1 for Bartenev–Khazanovich potential

Table 4.1 Critical values of relative contraction $\varepsilon_1 = 1 - \lambda_1$ for Bartenev–Khazanovich potential

β	1/8	1/4	1/2	1	10
$\varepsilon_1^{(1)}$	0.304	0.307	0.307	0.307	0.307
$\varepsilon_1^{(2)}$	0.035	0.089	0.168	0.242	0.306
$\varepsilon_1^{(3)}$	0.010	0.039	0.117	0.224	0.306

and 4.12). This is clearly demonstrated in Table 4.1, which gives the values of relative critical (limit) contraction parameters ${\varepsilon_1}^{(1)} = 1 - {\lambda_1}^{(1)}$ and ${\varepsilon_1}^{(2)} = 1 - {\lambda_1}^{(2)}$ at which the local loss of material's stability occurs under compression along two parallel coaxial cracks (values ${\varepsilon_1}^{(1)}$ correspond to the symmetric form of stability loss, and ${\varepsilon_1}^{(2)}$—to the antisymmetric (bending) form of stability loss). As can be seen, in the entire range of β change, the values ${\varepsilon_1}^{(2)} < {\varepsilon_1}^{(1)}$, i.e., stability loss for this material takes place according to the bending form. It is also seen that at small distances between cracks their mutual influence results in a significant decrease of critical compression parameters. Yet, with increasing distance between cracks, the relative critical contraction parameters tend to the value of $\varepsilon_1 = 0.307$, which for Bartenev–Khazanovich potential corresponds to the critical (limit) contraction parameter in the case of a single isolated crack in an infinite body (Guz et al. 1992, 2020). Besides, this table shows the values of ${\varepsilon_1}^{(3)}$, which are relative critical contraction parameters obtained from the solution of the axisymmetric problem on compression of a semi-bounded body containing a near-surface crack.

For mode III cracks, when the crack faces are under load (4.77), Fig. 4.15 shows the dependences of the ratios of stress intensity factors K_{III}/K_{III}^{∞} (where K_{III}^{∞} is determined from (4.78)) on initial stress parameters λ_1 for different values of geometric parameter β, which proves a significant influence of initial stresses on the *SIF* K_{III}. In this case, however, there are no effects of the resonance change of the stress intensity factor, as opposed to the problems on mode I and mode II cracks, since, evidently, under compression of the material containing two parallel cracks there is no stability loss corresponding to the torsion problem.

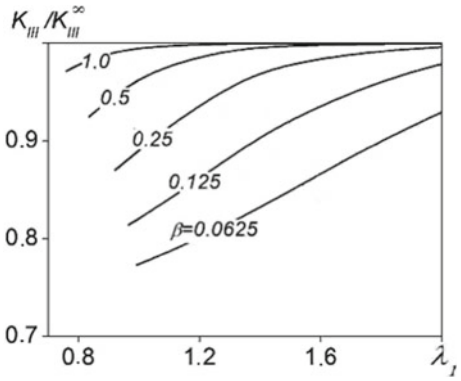

Fig. 4.15 Dependence of *SIFs* ratios $K_{III}/K_{III}{}^{\infty}$ on elongation (or contraction) ratio λ_1 for Bartenev–Khazanovich potential

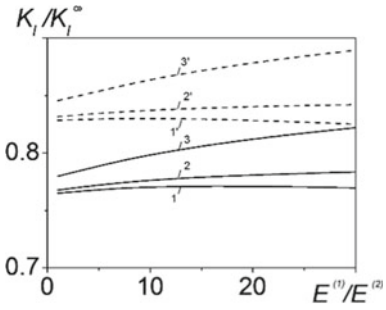

Fig. 4.16 Dependence of *SIFs* ratios $K_I/K_I{}^{\infty}$ on the ratio of elastic moduli $E^{(1)}/E^{(2)}$ for a laminated composite

Laminated two-component composite with isotropic layers (in macrovolumes, that is a transversely isotropic medium (Khoroshun et al. 1993)*, a compressible body, non-equal roots)*. For this material, the results of studying the axisymmetric problem of a pre-stressed body containing two parallel coaxial mode I cracks are presented.

Figure 4.16 shows that the ratios of stress intensity factors $K_I/K_I{}^{\infty}$ increase monotonously with the increase in the ratios of elastic moduli of the materials containing composite layers $E^{(1)}/E^{(2)}$ (the materials of the layers have identical Poisson's ratios $= 0.3$). Besides, it can be seen that for the values of dimensionless half-distance between the cracks $\beta = 0.25$ the corresponding values of $K_I/K_I{}^{\infty}$ (solid lines) are smaller than for $\beta = 0.5$ (dashed lines).

Figure 4.17 illustrates the dependence of the ratio $K_{II}/K_I{}^{\infty}$ on $E^{(1)}/E^{(2)}$. In Figs. 4.16 and 4.17, lines *1* and *1'* correspond to $\lambda_1 = 0.99$ (compressive initial stresses), lines *2* and *2'*—to $\lambda_1 = 1.0$ (no initial stresses), lines *3* and *3'*—to $\lambda_1 = 1.05$ (tensile initial stresses).

Figure 4.18 shows the dependence of the $K_I/K_I{}^{\infty}$ ratios on the glass concentration factor c_1 for different values of initial stress parameters λ_1, demonstrating the influence of initial stresses and mechanical characteristics of the composite on the values of stress intensity factors in the composition of aluminum/boron/silicate glass layers with those of epoxy/maleic resin.

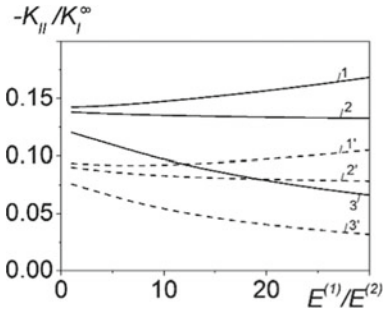

Fig. 4.17 Dependence of *SIFs* ratios $K_{II}/K_I{}^{\infty}$ on the ratio of elastic moduli $E^{(1)}/E^{(2)}$ for a laminated composite

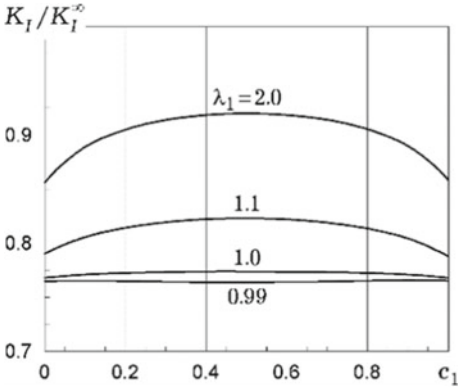

Fig. 4.18 Dependence of *SIFs* ratios $K_I/K_I{}^{\infty}$ on the glass concentration factor c_1 for aluminum/boron/silicate glass in epoxy/maleic resin

4.7 Conclusions

The results obtained in the research of the stress-strain state of pre-stressed materials containing near-surface cracks and two parallel coaxial cracks suggest the following conclusions:

- the order of singularity in the distribution of stresses in the vicinity of near-surface crack edge in a pre-stressed semi-bounded body and near the edges of parallel coaxial cracks in a pre-stressed unbounded body is equal to $-1/2$, i.e., it coincides with the order of singularity in the distribution of stresses near crack edges in the bodies free of initial stresses (Kassir and Sih 1975);
- in all the problems considered (with the exception of problems on torsion) a dramatic resonance change of stress intensity factors occurs when initial compressive forces approach the values corresponding to the local loss of material's stability in the vicinities of cracks, which permits the critical (limit) compression parameters to be determined directly from the solutions of corresponding non-homogeneous problems of the fracture mechanics of pre-stressed materials;
- the mutual influence between the crack and the half-space boundary (a near-surface crack) or between the cracks (two parallel cracks) causes a quantitative change (especially significant for small distances between cracks or between the crack

and the half-space boundary) in the values of stress intensity factors as compared to those obtained for an isolated crack in an infinite body. On the other hand, with an increase of the distance between the cracks (or the crack and the half-space boundary) the abovementioned influence gradually becomes weaker, and the values of stress intensity factors tend to the corresponding values obtained in the case of an isolated crack in an infinite material;

- the mechanical characteristics of materials produce a significant influence on the values of stress intensity factors;
- the critical (limit) compression parameters corresponding to the local loss of material's stability in the vicinities of cracks significantly depend on the geometric parameters of the problems (crack radii, distances between cracks, or those between the crack and material's boundary) and on the mechanical characteristics of materials.

References

Ainsworth RA, Sharples JK, Smit SD (2000) Effects of residual stresses on fracture behaviour - experimental results and assessment methods. J Strain Anal Eng Des 35(4):307–316

Bartenev GM, Khazanovich TN (1960) The law of high elastic deformation of network polymers. Vysok Soedinyeniya 2(1):21–28

Bateman H, Erdelyi A (1953) Higher transcendental functions. McCrew-Hill, New York

Bogdanov VL (2007) On a circular shear crack in a semiinfinite composite with initial stresses. Mater Sci 43(3):321–330

Bogdanov VL (2010) Influence of initial stresses on fracture of composite materials containing interacting cracks. J Math Sci 165(3):371–384

Bogdanov VL (2012) Influence of initial stresses on the stressed state of a composite with a periodic system of parallel coaxial normal tensile cracks. J Math Sci 186(1):1–13

Bogdanov VL, Guz AN, Nazarenko VM (2015) Nonclassical problems in the fracture mechanics of composites with interacting cracks. Int Appl Mech 51(1):64–84

Bogdanov VL, Guz AN, Nazarenko VM (2017) Unified approach in non-classical problems of fracture mechanics. LAP LAMBERT Academic Publishing, Saarbrücken [in Russian]

Bogdanov VL, Nazarenko VM (1994) Study of the compressive failure of a semi-infinite elastic material with a harmonic potential. Int Appl Mech 30(10):760–765

Bolotin VV (1994) Stability problems in fracture mechanics. Wiley, New York

Bolotin VV (2001) Mechanics of delaminations in laminate composite structures. Mech Compos Mater 37(5):367–380

Broutman LJ, Krock RH (1974) Mechanics of composite materials. In: Sendeckyj GP (ed) Composite materials, vol 2. Academic Press, New York

Cherepanov GP (1979) Mechanics of brittle fracture. McGraw-Hill, New York

Dvorak GJ (2000) Composite materials: Inelastic behaviour, damage, fatigue and fracture. Int J Solids Struct 37(1–2):155–170

Guz AN (1980) Theory of cracks in elastic bodies with initial stress - formulation of problems, tear cracks. Sov Appl Mech 16(12):1015–1024

Guz AN (1981) A criterion of solid body destruction during compression along cracks (two-dimensional problem). Dokl AN SSSR 259(6):1315–1318

Guz AN (1982) On the criterion of brittle fracture of materials with initial stresses. Dokl AN SSSR 262(2):285–288

Guz AN (1991) Brittle fracture of materials with initial stresses. In: Guz AN (ed) Nonclassical problems of fracture mechanics, vol 2. Nauk. Dumka, Kyiv [in Russian]
Guz AN (1999) Fundamentals of the three-dimensional theory of stability of deformable bodies. Springer, Berlin-Heidelberg-New York
Guz AN (2014) Establishing the foundations of the mechanics of fracture of materials compressed along cracks (review). Int Appl Mech 50(1):1–57
Guz AN (2021) Eight non-classical problems of fracture mechanics. In: Advanced structure materials, vol. 138. Springer, Cham
Guz AN, Bogdanov VL, Nazarenko VM (2020) Fracture of materials under compression along cracks. In: Advanced structure materials, vol. 138. Springer, Cham
Guz AN, Dyshel MS, Nazarenko VM (1992) Fracture and stability of materials with cracks. In: Guz AN (ed) Nonclassical problems of fracture mechanics, vol. 4, book 1. Nauk. Dumka, Kyiv [in Russian]
Guz AN, Nazarenko VM, Bogdanov VL (2013) Combined analysis of fracture under stresses acting along cracks. Arch Appl Mech 83(9):1273–1293
John F (1960) Plane strain problems for a perfectly elastic material of harmonic type. Commun Pure Appl Math 13(2):239–296
Kachanov LM (1988) Delamination buckling of composite materials. Kluwer Academic Publisher, Boston
Kassir MK, Sih GC (1975) Mechanics of fracture, vol 2. Three-dimensional crack problems. Noordhoff International Publishing, Leyden
Khoroshun LP, Maslov BP, Shikula EN, Nazarenko LV (1993) Statistical mechanics and the effective properties of materials. In: Guz AN (ed) Mechanics of composite materials, vol 3. Nauk. Dumka, Kyiv [in Russian]
Kienzler R, Herrmann G (2000) Mechanics in material space with applications to defect and fracture mechanics. Springer, Berlin
Malmeister AK, Tamuzh WP, Teters GA (1980) Strength of polymer and composite materials. Zinatne, Riga [in Russian]
Nazarenko VM, Bogdanov VL, Altenbach H (2000) Influence of initial stress on fracture of a half-space containing a penny-shaped crack under radial shear. Int J Fract 104:275–289
Prudnikov AP, Brychkov YA, Marichev OI (1986) Elementary functions. In: Integrals and series, vol. 1. Gordon and Breach Science Publisher, New York
Prudnikov AP, Brychkov YA, Marichev OI (1986) Special functions. In: Integrals and series, vol. 2. Gordon and Breach Science Publisher, New York
Shul'ga NA, Tomashevskii VT (1997) Process-induced stresses and strains in materials. In: Guz AN (ed) Mechanics of composite materials, vol 6. ASK, Kyiv [in Russian]
Uflyand YS (1977) Integral transformations in problem of the theory of elasticity. Nauka, Leningrad [in Russian]
Watson GN (1995) A treatise on the theory of Bessel functions. Cambridge University Press, Cambridge
Wu CH (1979) Plane-strain buckling of a crack in harmonic solid subjected to crack-parallel compression. J Appl Mech 46:597–604